Università degli studi di Padova

Dipartimento di Ingegneria Industriale

Corso di Laurea Magistrale in
Ingegneria dei Materiali

Extensive reuse of waste glasses in geopolymer-like material

Autore:

Riccardo Cavinato

Relatore:

Enrico Bernardo

Anno Accademico 2019/2020

Contents

List of Figures

List of Tables

Abstract

The present work investigates the possibility of realizing cementitious material re-using waste soda-lime glass. Whereas the material may contain small polymeric, metallic and ceramic contamination, it couldn't be remelted without influence on the quality of new glass product. This contaminated cullets could be used to realize geopolymer-zeolite material by low-temperature consolidation if activated with alkaline solution.
Two types of soda-lime glass powder were used, normal (non treated) and pre-washed with acid treatment, to form the geopolimerization blend with sodium aluminate solution. The study was conducted to analize the changing in the material with the variation of concentration of alkaline activator from 45% to 25% of $NaAlO_2$. Geopolymer-zeolite material were formed during curing time at 75 °C and kept in oven for a week to favor the consolidation. Two types of crystalline zeolites are generated: Zeolite Na-A (LTA) and Hydrosodalite; with their amount depends by the raw materials used. Those cementitious material were used also as binder in addition of coarse glass particles realizing a conglomerate. This combination allows to obtain an increase in the mechanical performance like particulate composites.
Microstructural and mechanical tests were conducted to understand the changing in the materials with the variation of alkaline concentration, raw materials used and with addition of coarse glass reinforcement. From the concentration point of view, the results show a reduction in the performance, sign of a minor degree of geopolymerization reaction. The results confirmed the previous works that were made on the other geopolymer material for construction field in substitution of ordinary Portland cements. The reuse of soda-lime waste glass, otherwise landfilled, gives additional value to our work which follows a vision of more sustainable economy.

Sommario

Il presente lavoro di tesi affronta lo studio della possibilità di realizzazione di materiale cementizio derivante da rifiuto vetroso. Tale materiale si presenta inadatto per la produzione di nuovi prodotti vetrosi, vista la presenza di contaminazioni polimeriche, metalliche e ceramiche derivanti dalla fase di riciclo. Il rifiuto di vetroso grezzo può essere utilizzato per realizzare un materiale geopolimerico-zeolitico per consolidazione a bassa temperatura mediante attivazione alcalina.
Sono state utilizzate due tipologie di polveri vetrose, polvere di vetro soda-lime e polvere di vetro soda-lime trattata con soluzione acida, che sono state unite alla soluzione di sodio alluminato per formare la miscela di reazione. Lo studio è stato condotto analizzando i cambiamenti del materiale al variare della concentrazione dell'attivatore ($NaAlO_2$) nella soluzione alcalina. Il materiale geopolimerico-zeolitico è stato mantenuto in forno alla temperatura costante di 75°C per una settimana per permettere il consolidamento della miscela. All'interno della gelo di geopolimero si sono formate due tipologie di fasi zeoliche cristalline: Zeolite Na-A (LTA) e Hydrosodalite, le cui quantità dipendono dalla polvere di vetro utilizzata.
Insieme materiale cementizio realizzato sono state anche unite particelle grezze di vetro come aggregato per formare un coglomerato. Questa combinazione ha permesso di realizzare dei manufatti con prestazioni meccaniche superiori, come per i compositi rinforzati con particelle.
Sono stati effettuati test microstrutturali e meccanici per capire l'influenza sul materiale del cambiamento della concentrazione di attivatore, della materia prima utilizzata e dell'aggiunta degli aggregati. I risultati raccolti confermano i lavori di studio effettuati su materiali geopolimerici realizzati per il settore costruttivo in sostituzione del cemento Portland comune. Il riutilizzo di rifiuto vetroso di soda-lime, altrimenti interrato visto la sua impossibilità di lavorazione, rende interessante questo lavoro in un'ottica di sviluppo economico secondo un ciclo produttivo più sostenibile.

Chapter 1

Introduction

Processing of waste glass is one of the crucial part of waste management of an increasingly less sustainable economy. Respect to other material, more than quarter of total amount of waste glass remains unaddressed [1] mostly because of composition and difficulties emerging during processing of fine cullet in which heterogeneous impurities are concentrated [2]. For that reason, exists a discrepancy between theoretical energy savings and their comparison with other materials. Using recycled glass could lead an energy saving respect 'virgin material' product only of 25%, whereas for aluminum the amount approaches 90%. A lot of energy is required for recycled material to be of the same quality of that from extracted raw materials, most of this energy is due to complicated sorting step of the cullet. A new beneficial way of waste processing could encourage development for manufacturers in glass recycling and reduce the amount of landfilled waste. Our approach is based on the valorization of discarded glass (starting from common soda-lime waste) used to realize product with added value [43].
First attempts to reuse glass waste have been made producing glass foams for thermal and acustic insulation, and marble-like glass-ceramics. Those materials are based on low temperature viscous flow (without remelting) but still implying a firing step with temperature in the range of 800 °C / 1000 °C. Our study is based on a non-firing production way with the focus on a non-fired ceramics: geopolymer. First attempts of geopolymer production using recycled materials was made with fly-ash coming from coal treatment, and little amount of glass waste as silica and alumina provider. In our case

was used only soda-lime glass powder with activation solution to favor the condensation of alumino-silicate hydrated.

1.1 Enviromental impact

Recycled glass is the by-products of crushed, mixed bottles and other glass stuff coming from selection of municipal and industrial waste. Glass is categorized as material under natural environmental states and can be recycled in a range of techniques sans affecting its chemistry. However waste glass management and its disposal is the subject of significant global concern, considering that the contemporary practice is still dump the non-recyclable glass in landfills. Whereas the material is non-biodegradable, these aren't an environmental and sustainable solution. In 2019 the world deposited estimates for glass are over 46 millions tons per year and by 2025 could reach 77 millions tons [3]. However for all the waste glass that are recyclable and able to reuse in glass factories, the problem of variation among the quality and color still remain. One challenge in the context of diverse glasses of dissimilar colors and origin is that they result out of control in the final product and can not be recycled and this is the core reason to dispose of it off to landfills. In case waste glass is collected in mixed type, secondary application of recycled materials is developed like glass wool, water filtration media and abrasives while another significant way to dispose is in construction conglomerate.
Geopolymer cement can be an environmentally substitute for conventional concrete. Application of such diverse waste for making geopolymer materials can deliver an optimistic environmental impact and energy saving, carbon mitigation and waste recycling objectives can also be achieved. One of the most attractive way of waste disposal management through its reuse it's blending with building conglomerate either as aggregates or as a supplementary cementitious material in concrete for the construction and infrastructure industries. The main component of glass is SiO_2 (greater than 70%) gives importance to its pozzolanic nature as a reactive aggregate in concrete manufacturing. However, this high silica content results in a comparatively poor percentage of aluminum. To ensure the development of

geopolymers and zeolites its necessary to raise the composition of the latter through adding up of a definite quantity of materials which are rich in reactive alumina. Waste glass has a propensity to dissolve and furnish condensable silanol groups owing to its chemical unsteadiness in alkaline media, piloting to the development of Silica rich gel which influences the attributes of the concluding product. At low temperature, glass fine particle react over time with an alkaline solution and bind the geopolymeric paste to good quality on interface. The recycle of waste glass powder into alkali-activated cement exploits its chemical instability in alkaline conditions and higher content of silica rich glassy phase. This characteristics encourage the alkali activation reaction converting it in a material that could substitute fly ash in the production of alkali activated cement. The feasibility of addition of waste glass coarse particle as aggregates in geopolymer concrete, increase the concept of sustainability of material in terms of revaluate waste materials.

Nowadays, the interest of the researchers is focalized on a trend towards less energy-intensive, green, innovative, affordable, sustainable, user-friendly materials with low carbon footprint. The production of ordinary Portland cement (OPC) involves high temperature reaction and high energy demand contributing at almost 8% of global CO_2 emission. It is not only consuming non-renewable minerals like Coals to obtain elevated temperature through their burning up necessitated for Calcination of raw material, but also found accountable to global warming and earth heating, which is the gigantic dilemma the present world is facing in this millennium. On the other hand, there are copious diverse waste like glass, from various sources laying in landfills creating health hazards and contaminating soils, air, surface and subsurface waters owing to their non-biodegradable chemistry. The European commission with Horizon 2020 EU Framework Programme for Research and Innovation have taken it as precedence to deliver affordable, innovative and viable technological ways for energy competence for building envelopes [4]. The development of new sustainable type of construction materials is fundamental if the construction sector wants to reduce the environmental footprint of its activities, which is incurred particularly through the production of Portland cement. One type of non-Portland cement that

is attracting particular attention is based on alkali-aluminosilicate chemistry, including the class of binders knows as geopolymers [5]. The main binding phases are derived by the reaction of aluminosilicates sourced with an alkaline solution that induces the formation of strong, insoluble binding phases. In facts, geopolymers possesses comparable or better performances than those of classic construction materials. Thanks to their capability to harden at low temperature, they allow to reduce the CO_2 emissions derived by traditional treatment of construction materials [6]. The CO_2 savings achieved by the use of alkali-activated material binder are mainly due to avoidance of carbonate precursors and the high temperature processing of all the cement constituents in a fossil fuel-fired kiln. Moreover, the use of inorganic waste like glass, otherwise landfilled, replacing metakaolin in the formulation of the product, gives another advantage in terms of reducing the CO_2 emission. The valorization of waste material in addition to lower CO_2 emission of the process, gives great importance to the research and the use of geopolymer as sustainable construction material. The difficulties for this application is based on the lack of certainty about the technical performances of recycled aggregates, consistency of properties, porosity and the presence of chlorides and sulphates [7]. The use of waste glass as aggregates of geopolymer cement is very eye-catching for the management and reduction of solid waste and the conservation of finite natural non-renewable resources.

It is possible to evaluate the differences between types of construction materials using CES Eduram 2018 to make Ashby diagram on CO_2 primary footprint. Ordinary Portland cement (OPC) has traditionally been used as binder phase in concrete, however OPC has high embodied energy with carbon dioxide equivalent ranging from 0,66 to 0,82 kg of CO_2 emitted for every kilogram produced [8]. The contribution of the production of OPC is approximately 8% of global anthropogenic CO_2 emission. The reasons of those high emissions have been attributed to: calcination of limestone which leads to formation and release of CO_2, and high energy demands during heating in rotary kiln at temperature greater than 1400°C. The range of reported carbon dioxide equivalent values of the alternative geopolymer cement is wide, with an estimation of 80% less than OPC and 25/45% lower than

OPC concrete. The difference in CO_2 emissions arise from: whether the mining, processing and transport of raw materials have been considering, and whether the energy expended during manufacturing of the alkaline activators is included in the estimates. In the figure 1.1 is reported the Ashby diagram related to CO_2 footprint of primary production and compressive strength for common construction materials. The data of CO_2 footprint assumed for our materials are derived by the previously consideration on the impact of geopolymer cement that has intrinsic differences, first of all the raw material. This graph can be used for an initial evaluation of the environmental impact of different materials, a more precise estimate should be made considering the raw material, energy consumption and production cycle.

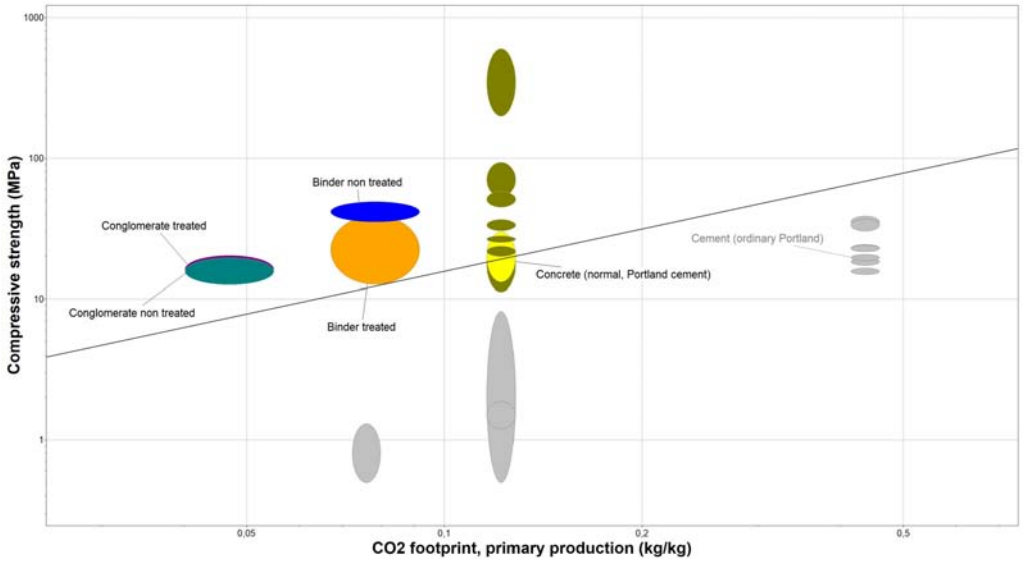

Figure 1.1: Ashby diagram for CO_2 footprint / Compression strength

1.2 Geopolymer and zeolite

The geopolymer-zeolite system has become interest in the construction field, such hybrid materials, depending on the material selection and processing, connect the advantageous properties of geopolymer as strong and durable binder, and zeolite with high surface area, porosity and adsorption capacity [9]. Geopolymers are general recognize as alkali-activated aluminosilicates, they may be considered as inorganic system composed by reactive solid source of SiO_2 and Al_2O_3 and alkaline activation solution [10]. One of the main interest behind the geopolymer is due to the utilization of industrial by-products, like fly-ash and glass wastes, for the synthesis of materials that can be applied for different purposes. A final solid material possesses region varying in degrees of crystallinity to fully amorphous. Their high chemical and fire resistance as well as relatively high mechanical strength gives those materials adapt to be used as construction and building materials, with a prospect of being an environmental-friendly substitute of ordinary Portland cement. Another important application of geopolymers is the absorption of heavy metals, which is the result of porous structure and the presence of negative charges in aluminum tetrahedra [45].
The formation of this hybrid material is due to the geopolymerization reaction that involves several steps like dissolution of precursors, re-orientation and condensation of the final products. Geopolymers are presented as amorphous gel that contain a percentage of unreacted materials as well as newly formed crystalline phases called zeolites. Alkaline ions, like Na+ and Ca+, embedded in the cavities of the network, allow the tetrahedrical coordination of aluminum ions with oxygen resulting the same structural unit like silicon tetrahedra [11]. This "two parts" geopolymer-zeolite materials connect the propreties of both constituent, exhibiting synergistic effect. The inter-connected and multiscale distributed pores of the network is a combination of zeolite microporosity and geopolymer meso and macropores. The effect of zeolite crystals formation in the matrix of geopolymer, which serves as strong support, results favorable for the application like monolithic membrane or building binder. To form the zeolitic crystals from raw materials is necessary hydrolysis of amorphous phase, which requires an alkaline re-

action system, high solution/solid ratio and temperature above 50°C. The formation of zeolites in geopolymer gel is often an accompanying to geopolymerization, and the type and amount of zeolite is correlated by the chemical composition of raw materials, the type of alkaline activator as well as curing condition.

- Role of Si/Al ratio: one of the most important factor that governs the possibility of formation of zeolitic phase during geopolymerization is the molar ratio of silicon to aluminum in reaction system. In general, the composition of zeolites is close to the composition of the gel from which they crystallize.

- Role of activator: the role of alkaline activator in the process of geopolymerization and in particular in zeolites formation, is rather complex and depend by the raw materials and activating solution used. In general the dependence of zeolite type on system alkalinity is related to the fact that some building units of the structure remain stable under different alkalinities. In case of alumino-silicate geopolymeric gel derived by alkali aluminate solution, at Si/Al ration of 1.0, the pH was a crucial factor in terms of zeolites crystallization.

- Role of curing: another parameters that influence the geopolymerization, and is related directly with other two, is curing. Different temperatures of activation result in the formation of various zeolitic pahses. In our case this parameter is irrelevant because the temperature of curing is constant for different samples that are prepared, so this aspect doesn't influence the zeolitic formation.

The mechanism of transformation from liquid precursor to dense "solid" gel results critical and needs a precise explanation. Alkaline activation solution controls the rate of structural reorganization and densification during geopolymerization. Lability influences the gels structure: greater lability allows extensive gel reorganization and densification resulting in a microstructure comprising dense gel particles and large interconnecting pores, whereas reduced lability promotes a decreased localized gel density and distributed porosity [12].

The geopolymeric gel is often considered as zeolite-like phase, zeolite precursor, or metastable amorphous zeolites, unable to crystallize due to unfavorable condition. Zeolites, forming parallel to geopolymerization, can be obtained in the matrix of geopolymer as a direct product. Zeolites are crystalline, hydrated tecto-alumino-silicates with a specific framework structure, consisting of silica and alumina tetrahedra linked by oxygen atoms in the corners. The structure is more regular respect to geopolymer, and containing well-defined channels and chambers filled with ions and molecular water [44].
The principal zeolite structures found in our work are Zeolite Na-A(LTA) and Hydrosodalite represented in figure 1.3. Zeolite Na-A (LTA) possesses the so-called α-cage comprised of 8 cuboctahedra linked by 12 cuboids. Hydrosodalite has SOD-cage that is connected with six nearest neigh-boring SOD-cages by common T4-rings. Hydrosodalite β-cage frame is indicated by $[AlSiO_4]_6$, a basic unit forming the sodalite framework.

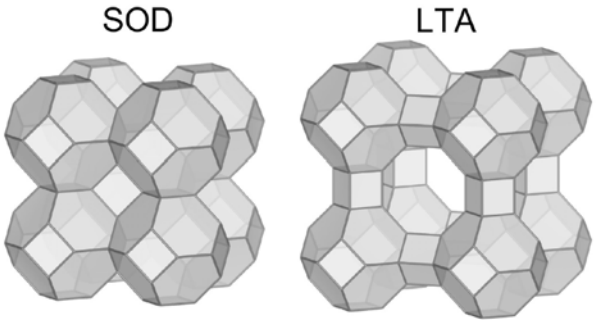

Figure 1.2: Zeolite structure of Hydrosodalite and Zeolite Na-A (LTA)

In 1950's the first model proposed to describe the mechanism for the alkali activation of materials was made by Glukhovsky. His study divides the process into three stages: destruction-coagulation, coagulation-condensation, condensation-crystallization. Based on this work, different authors have elaborated and extended the Glukhovsky theories applying the knowledge about zeolite synthesis in order to explain the geopolymerization process. Geopolymer structure is very similar to zeolite ones, and most authors agree that it involves a three step model of dissolution, orientation and hardening. Some authors claim that the exact reaction mechanism

of alkali-activated binders is not quite understood, although it depends on both type of raw materials an alkaline activator. Some model have been presented to describe the mechanism of zeolite formation in geopolymers. The transformation of amorphous aluminosilicate gel into zeolites is also determined by dissolution of raw materials, this is controlled by at least two processes [13]:

- Breakage of surface bonds due to solvent action and formation of soluble species that leave the surface of the dissolving solid
- Reaction of the dissolved species on/with the surface of the dissolving solid

The occurrence of solid phase transformation mechanism presumes the development of a polymerized hydrogel between silica and alumina following the crystallization condition. The work of Provis and Van Deventer confirmed that the initial geopolymer gel is transformed over time into a more ordered phase. With this considerations, is possible to define a model that describe the geopolymerization-crystallization mechanism of zeolite formation in several steps:

- Dissolution-hydrolysis: release of silica and alumina species under alkaline attack, this is fundamental for solid particles conversion into a geopolymeric gel. The dissolution at the surface, resulting in the liberation of aluminate and silicate into solution, has always been assumed to be the mechanism responsible for conversion of the solid during geopolymersization.
- Speciaton equilibrium: once in the solution with aqueous phase, the dissolved species form a complex mixture of silicate, aluminate and alumino-silicate species, and the speciaton equilibria within these solutions have been studied extensively
- Hydrolysis-polycondensation: dissolved species rapidly creates a supersaturated aluminosilicate solution which then form oligomers that constitute the gel. The gel generation happens simultaneously to setting and hardening of 3D aluminosilicate network due to polyconden-

sation. The resulting geopolymer gel has a zeolite-like structure. This process releases the water that plays the role of a reaction medium.

- Reorganization: after gelation the system continues to rearrange and reorganize, increasing the connectivity of the gel network
- Polymerization-crystallization: starts the ordering of three dimensional aluminosilicate network. During geopolymerization water acts as a reagent and also as a reaction by-product.

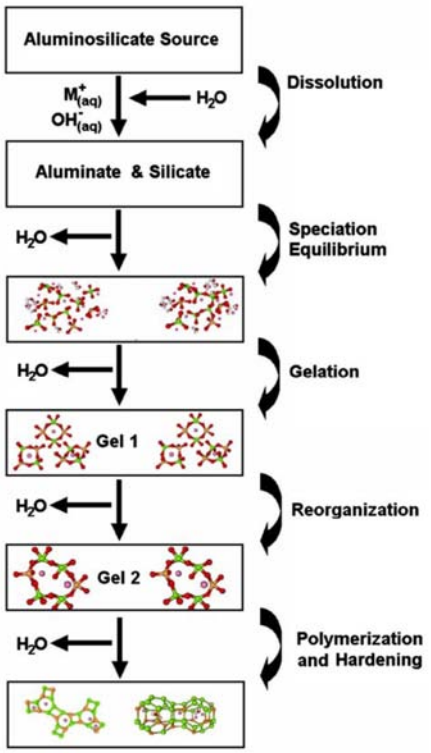

Figure 1.3: Geopolymerization mechanism for alumino silicate materials

Another model that describe the mechanism of formation of zeolite show that at first a stable ordered nanocrystal nucleus is formed in the geopolymer gel [14]. Polymerization and rearrange occur on the surface of the particles when alumina and silica tetrahedra are sufficiently concentrated close to the theoretical composition of a zeolite forming the ordered nanocrystalline core. With the transport of Si-O and Al-O "polymers" by water molecules, the nanocrystals gradually grow into zeolites.

1.3 Geopolymer-zeolite system as construction materials

Geopolymers are recently discovered inorganic materials with a wide range of application including heat-resistant coatings and adhesive as well as repair mortars with high acid-resistance and concretes with less environmental impact than conventional Portland cement-based material [15]. Based on great mechanical, microstructural and thermal properties, intensive studies focused on conventional geopolymer system have been made. In the case of construction materials, these are note as geopolymer cements, a group of alkali-activated materials produced by reactions between alkaline solutions and solid aluminosilicates [16].

The alkalis, introduced as activating solution, have an important role in geopolymerization reactions, initially they generate a sufficiently high pH to activate the aluminosilicate raw materials, and then balancing the charge of the growing aluminosilicate gel network [17]. The role of sodium, principally introduced in the mixture by the alkaline solution, essentially determines the extent of reaction and the densification of the microstructure. Water plays a critical role during geopolymersization, less water lead greater extent of crystallite formation which is in contrast with the phenomena that happens for "traditional" geopolymer system. This difference may be due to the rapid dissolution of the aluminate source and slower dissolution of silica in the early stage of geopolymersization [18]. The product of geopolymerization is amorphous gel sodium alumino-silicate hydrate (N-A-S-H). The first part of reaction produce an Al-rich gel gradually richer in silicon with the reaction progress, when more Si-O groups dissolve and concentration of silicon in the reaction medium rises [19]. The 3D structure of geopolymers consists of Si-O-Al framework with tetrahedra of silicon and aluminum sharing oxygen corners. The presence of calcium oxide in the mixtures can produce new type of gel that coexist with N-A-S-H, calcium silicate hydrate C-S-H and calcium alumino-silicate hydrate C-A-S-H. It was also suggested that at low alkalinities both N-A-S-H and C-S-H gels form, while at high alkalinities N-A-S-H is a predominant phase with some calcium precipitates. Despite the similarities in the molecular structure and nanostructure, the

differences in the properties of geopolymer derived from different raw materials are clearly evident. Although the inherent differences in the dissolution properties and phase composition result in geopolymers that exhibit different properties, it is observed that the same silicon and aluminum network, and the same gel-phase binder are present in both system [20]. The most used waste-derived material in geopolymer production consist of fly-ash, a by-product derived by coal fired-power plants [21]. Fly-ash as raw material is widely available worldwide and consists of an amorphous phase powder rich in alumina and silica [48]. The activation reaction typical of geopolymerization is due to sodium and potassium hydroxide solutions; for balance the silica content of the mixture, sometimes is used sodium or potassium silicate solution (water glass). Alternatively, is possible to substitute the silica source using waste glass (soda-lime glass coming from urban waste) instead of water glass, normally used as alkaline activator [22]. The reuse of waste glass as raw material for geopolymer production, provide extra environmental advantage because it avoids the energy demand and CO2 emission due to sodium silicate production, where the temperature required to melt sodium carbonate and silica mixtures are high [23]. Moreover could be an interesting way of reuse a fraction of glass currently landfilled, representing an economic advantage as well as environmentally friendly solution to the landfill problems. The gel binder structure formed by alkali activation of fly ash are highly cross linked by tetrahedral units N-A-S-H type. Crystalline zeolites and related phases also develop in these materials over a more extended curing time, with higher temperatures and higher water contents favoring the development of more crystallinity [50].
The main difference between an alkali-activated binder and a traditional Portland cement is that the hardening of Portland cement is induced simply by mixing with water that induced the hydration reaction, whereas alkali activation requires the addition of an alkaline component in aqueous solution. The development of alkali based cements has changed the research and production of classic building material. alkalis are generally thought of as the cause of deleterious alkali aggregate reaction, and the tendency has been to avoid any addition in Portland cement and commonly to require from the manufacturers the supply of low-alkali cements. On the contrary,

the addition of alkaline natural pozzolans (like sodium alumino-silicate) substantially reduce the alkali aggregate reaction of high alkaline cements. Geopolymer cements do not generate any dangerous alkali aggregate reaction, with no measured expansion of the product respect to the Portland cement that show an increase in the dimensions during hardening time [24].

Chapter 2

Materials and Methods

2.1 Raw materials

The principal raw material used for this study is Soda-lime glass coming from SASIL SRL, Biella, Italy, in the shape of powder (mean diameter 30 μm) and rough granulate with dimension comprised between 300 μm and 1400 μm. The composition of waste glass is reported in table 2.1.

SiO_2 %wt	Al_2O_3 %wt	Na_2O %wt	K_2O %wt	MgO %wt	CaO %wt	FeO %wt
71,6	1,0	13,5	0,4	3,9	9,0	0,1

Table 2.1: Soda-lime glass composition used as raw material

For the alkali solution has been used common demineralized water (DIW) and sodium aluminate $NaAlO_2$ powder coming from Sigma Aldrich, Gillingham, UK, with particle's size of 17 μm and degree of impurities $\leq$ 0,05% (in the case of Fe_2O_3).

2.2 Laboratory Instruments

Samples preparation has been made in laboratory using mechanical mixer with analog regulator for mixing rate, in order to control the blend procedure of raw materials and liquid solution.
The mineralogical analysis on the samples was execute by X-Ray diffraction with XRD Bruker D8 Advance, Karlsruhe, Germany - $CuK\alpha$ radiation, 0.15418 nm, 40 kV-40 mA, 2θ = 5 - 80°, step size 0.05° and 2 s counting time. The scattering of X-rays from atoms produces a diffraction pattern, which contains information about the atomic arrangement within the crystal. With the identification of diffraction peaks is it possible to analyze the atomic structure and microstructure of a sample. The diffraction peak position is recorded as the detector angle (2 θ) and are determined by the distance between parallel planes of atoms. Bragg's law calculate the angle where constructive interference from X-rays scattered by parallel planes of atoms will produce a diffraction peak. The value d is the distance between two parallel planes of atoms in the unit cell. The intensity of the diffraction peaks are determined by the arrangement of atoms in the entire crystal. The amplitude of scattered light is determined by: where the atoms are on the atomic planes, what atoms are on the atomic planes. For the determination of the phases was used "Match!" Software (Crystal Impact, GbR, Bonn, Germany), supported by data coming from PDF-2 database (ICDD-International Centre for Diffraction Data, Newtown Square, PA, USA).
The morphological and microstructural analysis was performed by Scanning electron microscopy (SEM, FEI Quanta 200 ESEM, Eindhoven, The Netherlands). SEM analysis is a powerful investigative tool which uses a focused beam of electrons to produce complex, high magnification images of a sample's surface topography. The machinery uses a focused beam of high-energy electrons to generate a variety of signals at the surface of solid specimens. The SEM is also capable of performing analyses of selected point locations on the sample. This approach is especially useful in qualitatively or semi-quantitatively determining chemical compositions, crystalline structure and crystal orientations.
NMR spectra in the solid state were obtained on a Varian 400 spectrometer

equipped with a narrow bore, triple resonance T3 Magic Angle Spin (MAS) probe spinning 4 mm rotors and operating at ^{1}H, ^{27}Al and ^{29}Si frequencies of 400.36, 104.32 and 79.53 MHz, respectively. The nominal temperature of the probe was always set to 298 K. Single pulse spectra were acquired at 10 kHz MAS with 800 scans for ^{27}Al and 12 kHz MAS with 1248 scans for ^{29}Si. The repetition delay was set to 2 and the chemical shifts were referenced against aluminium nitrate (^{29}Al) and Q8M (^{29}Si). An NMR instrument allows the molecular structure of a material to be analyzed by observing and measuring the interaction of nuclear spins when placed in a powerful magnetic field. The precise resonant frequency of the energy transition is dependent on the effective magnetic field at the nucleus. This field is affected by electron shielding which is in turn dependent on the chemical environment.

Mechanical tests were conducted on Galdabini 1890 Quasar 25 and Labtest software to managed the data. The study of compression strength was conducted using flat plate of the machine measuring the maximum force needed to break the sample, with load speed of 0,5 mm/min. The study of bending strength or MOR (modulus of rupture) was conducted using a three-point configuration with 16 mm of distance from base supports. The test was conducted follow the BS EN 12390-5:2019 normative of testing hardened concrete in order to obtain comparable data.

The study of elastic modulus of the materials was conducted with a non-destructive dynamic resonance testing using GrindoSonic Mk5 device. It is based on the "impulse excitation technique" with the object under testing subjected to an initial deformation by means of light mechanical impulse. The frequencies obtained were used to calculate the elastic modulus of the sample.

The geometric density was evaluated considering the mass to volume ratio of bulk samples. Instead, apparent and true density were measured by using a helium pycnometer Micromeritics AccuPyc 1330, Norcross, GA, using bulk and finely crushed samples.

2.3 Samples preparation

The sample preparation follow the same procedure for all the different types of binder material (treated and non-treated). This difference regards the treatment of the soda-lime powder before the start of the mixing procedure. Soda-lime powder were washed in aqueous solution kept stable at pH 5 and mixed for three hours. The pH of the solution was monitored with litmus test at regular interval and kept constant with dropwise addition of HCl. After the mixing in acid solution the powder treated needs to be washed by HCl remained with 6-times washing in demineralized water (DIW). What achieved was a suspension from which it's necessary to completely remove the remaining water. To do this, the glass acid suspension was dried at 40 °C a couple of days so as obtain only fine powder of soda-lime treated powder.
To produce the alkaline solution, sodium aluminate powder was mixed with demineralized water (DIW) for the time necessary to have uniform dispersion (about 15 minutes). In this phase the concentration of the activating element of the consolidation reaction was determined.
In all graphs and tables of this thesis, "$\%NaAlO_2$" indicates the concentration of alkaline activator ($NaAlO_2$) in the alkaline solution (DIW + $NaAlO_2$).
After that, the procedure of sample preparation was the same both for soda-lime powder treated and non-treated. The mixture was obtain by blending the sodium aluminate solution with soda-lime powder. The ratio solid / liquid of the mixtures has always been about 50 / 50 in order to have good miscibility during the stirring of the suspension. Only for binder samples with $NaAlO_2$ concentration of 35% the retio was decreased, but difficults were registered in the initial mixing of the blend. It was roughly considered in all the mixtures "solidus" the soda-lime powder part and "liquidus" the alkali solution, forgetting the solid part (sodium aluminate powder) that are present in the latter. Using a mechanical mixer, the mixture with soda-lime powder and sodium aluminate solution were mixed for 3 hours at 200 / 300 rpm. This procedure is delicate because to have a good suspension, is necessary to add little by little the powder to facilitate mixing with alkali

solution. The extended time was necessary for obtain a uniform suspension. Once the mixing phase was ended, the polystyrene container was closed with their cover (not a waterproof closing) and put into the oven at steady temperature of 75 °C and kept there for a week to favor the consolidation. Even if the container does not allow a watertight seal, no problems were recorded due to the drying gradient. During the curing time, there hasn't been observed sedimentation of the heavy species in the samples. That confirmed the rightness of the solidus/liquidus proportion and the uniformity obtain with the long time stirring. Almost all the solid powder material that were presented in the mixture, reacts with alkali solution, becoming the massive sample desired. After that, the liquid blend become a solid sample easily to extract form the plastic container because of the little amount of volumetric retire of the thick discs. Shape, dimension and mechanical characteristic of the sample remained unchanged during the time.

In table 2.2 were presented the composition for different samples of binder treated and non treated. The species were prepared in function of the percentage of $NaAlO_2$ in activation solution (DIW + $NaAlO_2$). Starting from 45% of $NaAlO_2$ in the solution, efforts have been made to reduce the amount of activator until 25% in the mixture. As said before, ratio between soda-lime powder and activator solution were kept constant for almost all the samples, except for the species at 35% of $NaAlO_2$ where it was tried to increase the solid / liquid ratio. This difference of 35% samples and the other, must be taken into account for the results and discussion chapter.

samples	SLG powder (g)	alkaline solution (g)	$NaAlO_2$ (g)	% $NaAlO_2$ in alkaline solution	$NaAlO_2$ ratio on total glass
binder non treated	15	15	6,75	45%	0,45
	15	15	6	40%	0,4
	40	35,5	12,4	35%	0,31
	15	15	4,5	30%	0,3
	15	15	3,75	25%	0,25
binder treated	15	15	6,75	45%	0,45
	15	15	6	40%	0,4
	40	35,5	12,4	35%	0,31
	15	15	4,5	30%	0,3
	15	15	3,75	25%	0,25

Table 2.2: Composition of binder non-treated and treated

The last column of the tables was dedicated to the ratio between $NaAlO_2$ and the total glass inserted in the mixtures. This value results important in terms of product's cost, because only sodium aluminate represents an expense for raw materials.
To produce conglomerate sample with soda-lime glass granulate inside, was used the same procedure used for binder with subsequent addition of raw material coarse particles before cured phase. The rough soda-lime granulate (same composition of the soda-lime powder) was milled to have the size suitable for the dimension of the samples. It was possible reduce the size with orbital mill in the range between 300 μm and 1400 μm. That granulate's dimension was taken to obtain a good filling of the aggregate in function of the size of the sample. With bigger product could be possible the use of bigger aggregates. After the mixing procedure of the binder, the SLG granulate was inserted using a vibrational mixer to homogenize the mixture. Then, the sample was put in the oven and cured for the same time of the binder's sample. In table 2.3 were presented the composition for different samples of conglomerate treated and non treated.

samples	SLG powder + granulate (g)	alkaline solution (g)	$NaAlO_2$ (g)	% $NaAlO_2$ in alkaline solution	$NaAlO_2$ ratio on total glass
conglomerate non treated	12 + 16	11	4,95	45%	0,176
	12 + 16	12	4,8	40%	0,171
	12 + 16	12	4,2	35%	0,15
	12 + 16	12	3,6	30%	0,128
	12 + 16	12	3	25%	0,107
conglomerate treated	12 + 16	11	4,95	45%	0,176
	12 + 16	12	4,8	40%	0,171
	12 + 16	12	4,2	35%	0,15
	12 + 16	12	3,6	30%	0,128
	12 + 16	12	3	25%	0,107

Table 2.3: Composition of conglomerate non-treated and treated

2.4 Equations

In this section are described the equations used to evaluate data coming from mechanical tests and density's study. Calculations were made using Excel and Matlab R2019b and the obtained values are indicated in tables presented in Chapeter 3, results and discussion

2.4.1 Elastic modulus

To calculate the elastic modulus from the characteristic frequency vibration measured with GrindoSonic Mk5, it was necessary to use a function that takes into account the geometrical and physical features. The sample acts as a spring-mass system and produce a transient mechanical vibration. The frequency of this vibration depends on the mass of the object and its stiffness, which is determined by its shape, dimension and the modulus of elasticity of the material.
The equation is:

$$E = \frac{0,9465 \cdot m \cdot f^2}{b \cdot \left(\frac{L}{t}\right)^3 \cdot T1 \cdot 10^6} \tag{2.1}$$

where:

- E is the elastic modulus, in GPa
- m is the mass, in g
- f is the characteristic frequency, in Hz
- b is the width of the sample, in mm
- L is the length of the sample, in mm
- t is the thickness of the sample, in mm
- T1 is a corrective factor in function of dimensions and poisson factor

2.4.2 Compression strength

The value of stress was obtained by the general compression formula:

$$\sigma_{comp} = \frac{F}{A} \tag{2.2}$$

where:

- σ_{comp} is the compression strength, in MPa (N/mm^2)
- F is the maximum load, in N
- A is the area of the sample, in mm^2

2.4.3 Bending strength

The flexural strength is given by the equation presents in the BS EN 12390-5:2019 normative:

$$\sigma_{bend} = \frac{3 \cdot F \cdot L}{2 \cdot b \cdot h^2} \tag{2.3}$$

Where:

- σ_{bend} is flexural strength, in MPa (N/mm^2)
- F is the maximum load, in N
- L is the distance between the lower rolled supports, in mm
- b is the width of the sample, in mm
- h is the height of the sample, in mm

.

2.4.4 Porosity

Porosity of our samples were calculated using three types of densities: ρ_{geom} (geometric), ρ_{app} (apparent) and ρ_{true} (true).

$$\rho_{geom} = \frac{m}{V} \tag{2.4}$$

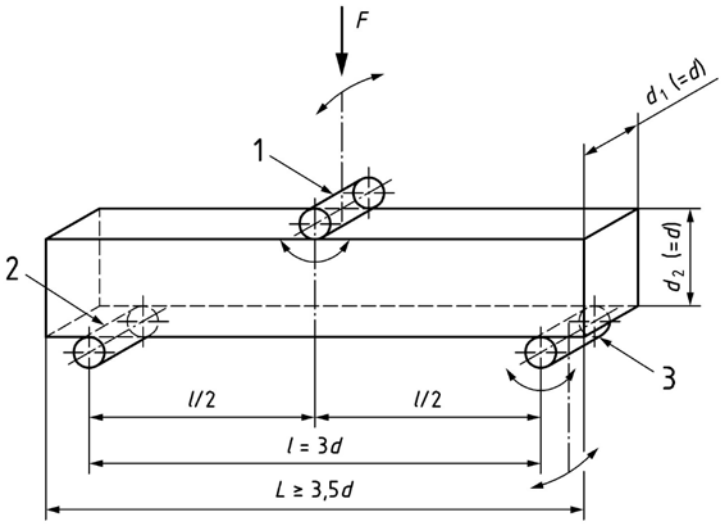

Figure 2.1: Three points BS EN 12390-5:2019 normative configuration

$$\rho_{app} = \frac{m}{V - V_{open}} \tag{2.5}$$

$$\rho_{true} = \frac{m}{V - V_{open} - V_{clos}} \tag{2.6}$$

Where:

- m is the mass of the sample, in g
- V is the volume of the sample, in mm^3
- V_{open} is the volume of open porosity, in mm^3
- V_{clos} is the volume of closed porosity, in mm^3

$$\frac{\rho_{geom}}{\rho_{app}} = 1 - f_{open} \tag{2.7}$$

$$\Phi_{open} = f_{open} \cdot 100 \tag{2.8}$$

Where:

- f_{open} is the open porosity factor

- Φ_{open} is the open porosity, in %

$$\frac{\rho_{geom}}{\rho_{true}} = 1 - f_{open} - f_{clos} \tag{2.9}$$

$$\Phi_{clos} = f_{clos} \cdot 100 \tag{2.10}$$

Where:

- f_{clos} is the open porosity factor
- Φ_{clos} is the open porosity, in %

Chapter 3

Results and Discussion

3.1 Mineralogical analysis, XRD

This section investigate geopolymer-zeolite materials produced from soda-lime glass powder and sodium aluminate solution. These materials contain a comparatively large fraction of crystalline zeolites, while conventional geopolymers are amorphous to X-rays and usually contain only minor frations of crystallite byproducts. A polycrystalline sample should contain many crystallites, therefore all possible diffraction peaks should be observed. For every set of planes, there will be a small percentage of crystallites that are properly oriented to diffract. Irradiating a larger volume of material can help ensure that a statistically relevant number of grains contribute to the diffraction pattern. X-ray diffraction Bruker D8 Advanced was used to study the mineralogy of the phases presented in the samples.
The XRD graph in figure 3.1 show the patterns of soda-lime glass powder non treated and treated. The amorphous nature of glass is indicate by the 'amorphous hump' centred at 25° with the characteristic peaks of quartz (PDF $\sharp 46-1045$), consistent with the above-mentioned contaminations of discarded cullet fractions. The difference between non treated and treated is evident in more pronounced peaks at 21° and 37°, while for the main peak at 27°, the intensity is almost the same for two powders [51].
For geopolymer-zeolite materials with concentration of alkaline activator of 45%, represented in figure 3.2, the reaction of soda-lime glass with activating agent is testified by the shifting of the 'amorphous hump'. Char-

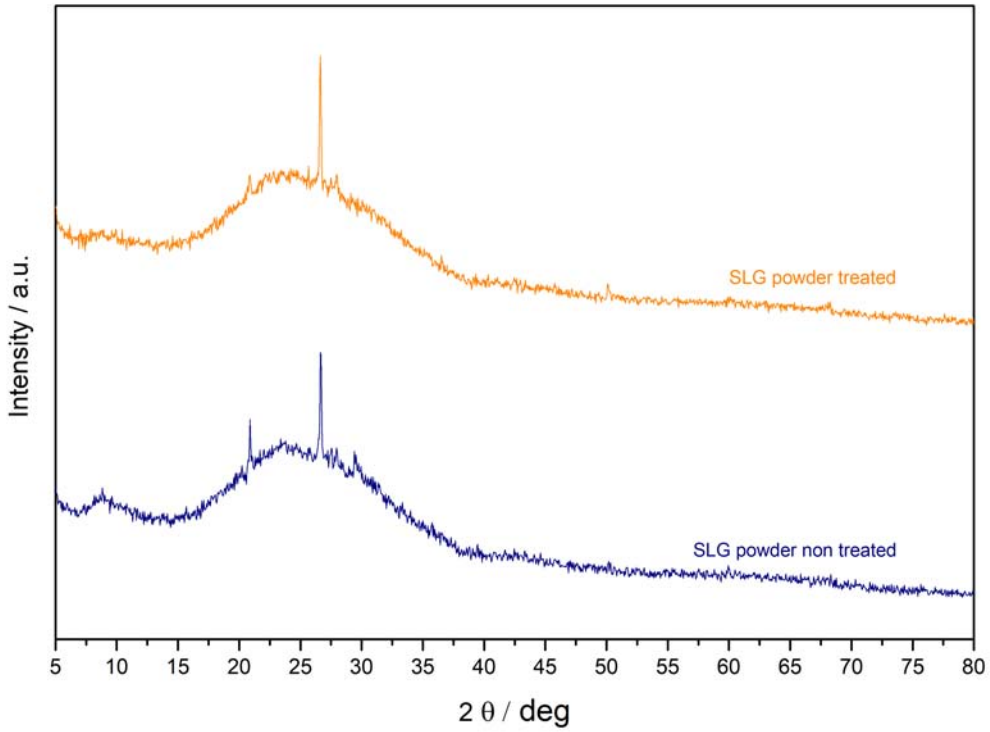

Figure 3.1: XRD soda-lime glass powder non-treated and treated

acteristic for silica-based glasses, at higher 2θ angles (known to be correlated, in a glass, with the incorporation of network modifiers [25], [26]) with a shift at 30° after the activation, which indicates the formation of amorphous geopolymeric gel. Hydrothermal alkaline reaction of soda-lime glass lead to the formation of zeolites with various frameworks depending on the reaction condition like temperature, alkali cation, Si/Al ratio etc. The main peaks present in the pattern are attributable to Zeolite Na-A (LTA) ($Na_{12}[(SiO_2)_{12}(AlO_2)_{12}]27 \cdot H_2O$, PDF ♯73 − 2340) and Hydrosodalite ($Na_8Si_6Al_6O_{24}(OH)_2]2 \cdot H_2O$, PDF ♯72 − 2329) crystals. In addition, low amounts non-reacted crystallite impurities of the silica, i.e. quartz (PDF ♯46 − 1045) and calcite (PDF ♯01 − 086 − 1045), were observed in the cured samples, indicating that these didn't participate to the reaction. The Zeolite Na-A is characterized by three dimensional cubic structure, as will observed in microstructural section. The silica to alumina ratio in Zeolite Na-A equals to 1 with the numbers of mobile Na equals to Al atoms.

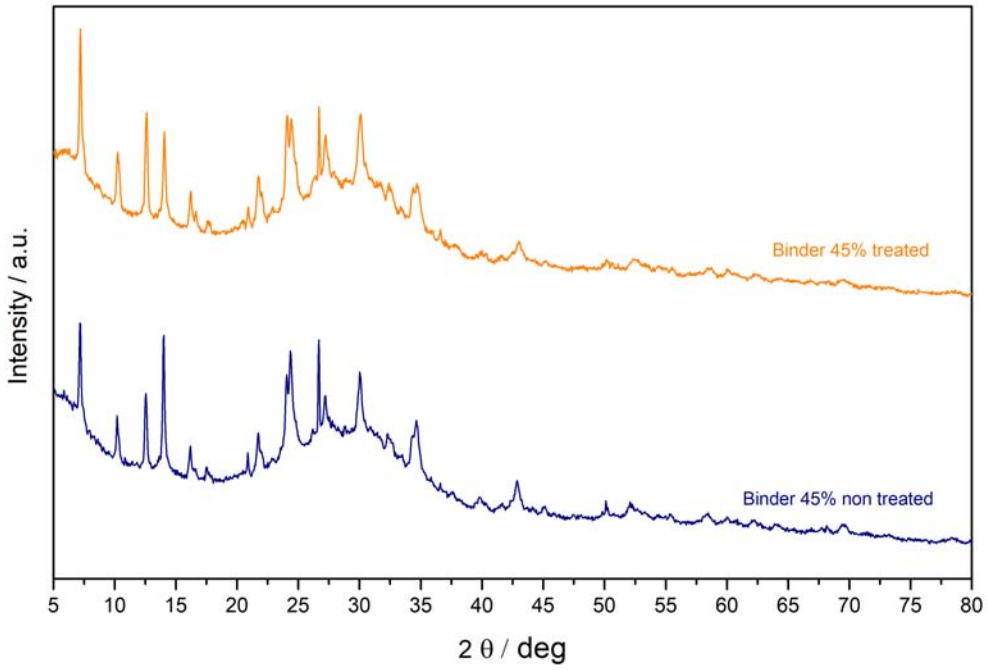

Figure 3.2: XRD binder 45% non-treated and treated

This means that possesses relatively high exchange capacities owing to their chemical structure [27].

The studies of Subotic and Graovac (1985) on the formation of Zeolite Na-A in hydrothermal condition showed that the reaction was governed by autocatalytic nucleation. The reaction of nucleation increases during the crystallization process because with formed aluminosilicate units, even the gel regions with ordered structure become potential nucleation sites [28].
A high water content allows a major hydration for the species in solution, with little influence of ion-pairing interaction. Although the silicate and aluminate species are largely determined by the concentration of alkali and by the Si/Al ratio in the solution, even the dilution allows the solution phase transport and reorganization. Nucleation centers in the mixtures are redly supplied with aluminosilicate species for growth by diffusion of dissolved glass molecules. With this condition the growth of precipitate occurs without steric hindrance and fully crystalline phase forms.
During the curing time in oven occurs the transition from apparently amorphous to partially crystalline. This phenomena of transition of ampor-

phous geopolymers to a well defined zeolite structure has also been observed through Si MAS NMR and SEM analysis which will be addressed later.
One of the first difference that is visible between the pattern in figure 3.2, is the formation of Zeolite Na-A that was enhanced by the use of pre-washed glass. This was expected, since acid attack is known to determine the removal of alkali ions from the glass surface, transforming it into a hydrated silica layer [29]. Instead, for sample non treated, Hydrosodalite main peak results more accentuated respect to Zeolite Na-A. The Na/Al/Si atomic balance in Zeolite Na-A (Na/Al/Si=1/1/1) effectively matches the hypothesis of equimolar reaction between $NaAlO_2$ and (hydrated) silica (1 $NaAlO_2$ + 1 SiO_2). This is in a good agreement with what was observed by Greiser et al. [30] in the geopolymer composites obtained from reaction between $NaAlO_2$ and silica fume. On the contrary, Hydrosodalite features an alkali excess Na+ (Na/Al/Si=4/3/3) that could be explained as the effect of inclusions in the binder, originating from $NaAlO_2$ and dissolved glass.
One-part geopolymers, synthesized from silica and sodium aluminate, yield Zeolite Na-A and Hydrosodalite as major crystalline reaction products, as well as geopolymeric gel. The relative amounts of the zeolites depend on the initial SiO_2/Al_2O_3 ratio, higher silicon oxide respect to aluminum oxide generally leads to a higher fraction of Zeolite Na-A. The sharpness of the zeolite peaks can be an indication of relatively large crystals. This could be the reason behind the higher intensity of the Zeolite Na-A peaks for the XRD pattern of lower concentration.

The differences in terms of types of zeolites formed, are reported in table 3.1 for Zeolite Na-A, and in table 3.2 for Hydrosodalite. As said before, the Zeolite Na-A was enhanced by the use of pre-washed powder and with lower

sample	45% $NaAlO_2$	40% $NaAlO_2$	35% $NaAlO_2$	30% $NaAlO_2$	25% $NaAlO_2$
binder non treated	12063	10352	16353	18613	25999
binder treated	14273	27842	16536	18014	28044
conglomerate non treated	13496	9524	8865	11638	12729
conglomerate treated	7434	13405	16419	7735	6663

Table 3.1: Main peaks Zeolite Na-A at $2\theta = 7, 18$

sample	45% $NaAlO_2$	40% $NaAlO_2$	35% $NaAlO_2$	30% $NaAlO_2$	25% $NaAlO_2$
binder non treated	11479	13462	8730	6818	6425
binder treated	9417	5632	6796	6192	5348
conglomerate non treated	5354	9735	8582	6519	5448
conglomerate treated	9128	5065	4915	4822	4916

Table 3.2: Main peaks Hydrosalite at $2\theta = 14,08$

concentration of sodium aluminate. Hydrosodalite will acts in reverse.

Although XRD is an analytical technique commonly used for investigation of geopolymer system, it is important to note that this technique has significant limitation due to the apparent amorphicity of these materials. In the following figures are presented the XRD pattern for all the samples: binder non treated (fig. 3.3), binder treated (fig. 3.4), conglomerate non treated (fig. 3.5) and conglomerate treated (fig. 3.6). In those graphs is interest to notice how the characteristic peaks of Zeolite Na-A ($2\theta = 7,18$) and Hydrosodalite ($2\theta = 14,08$), according to concentration of alkaline activator.

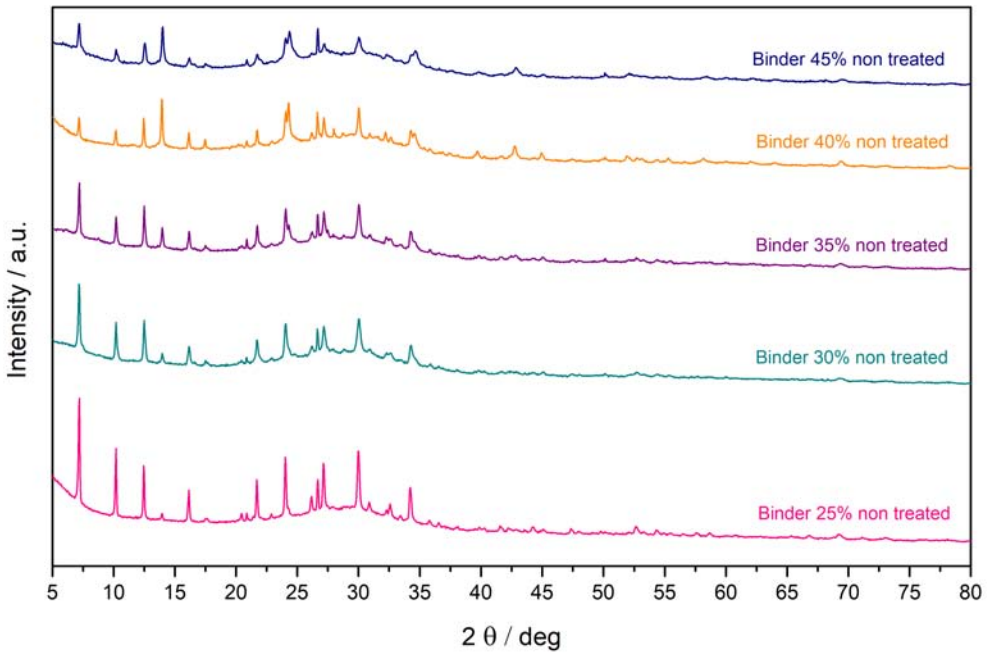

Figure 3.3: XRD binder non treated for each $NaAlO_2$ concentration

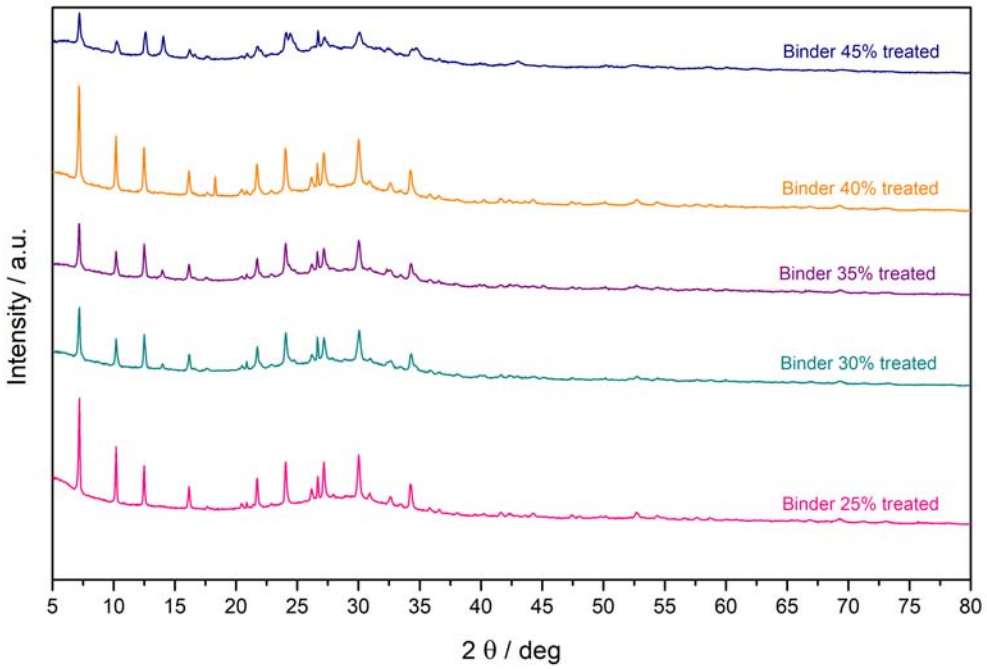

Figure 3.4: XRD binder treated for each $NaAlO_2$ concentration

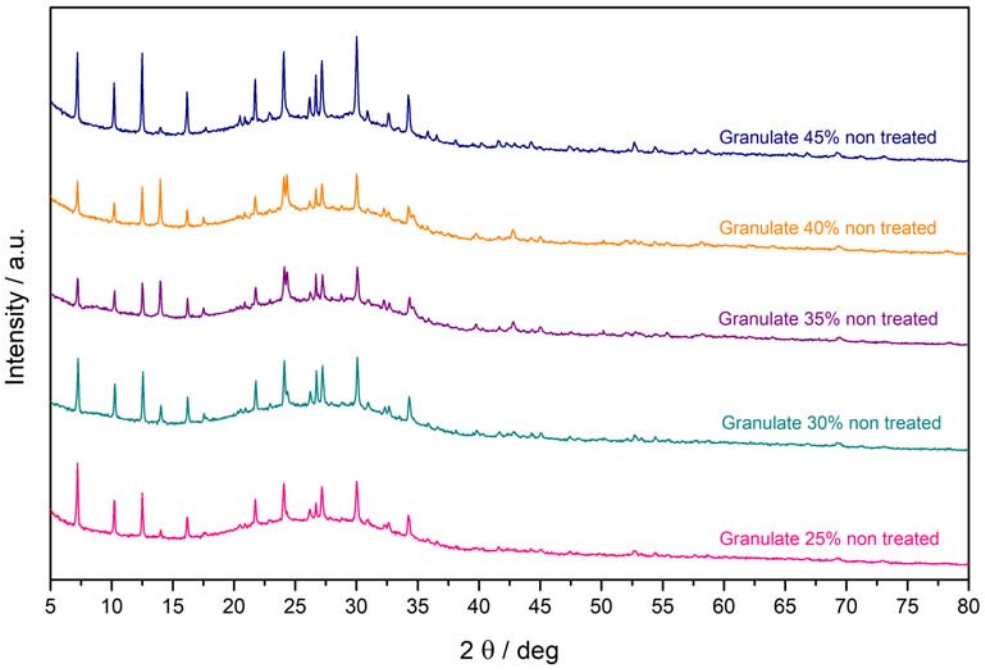

Figure 3.5: XRD conglomerate non treated for each $NaAlO_2$ concentration

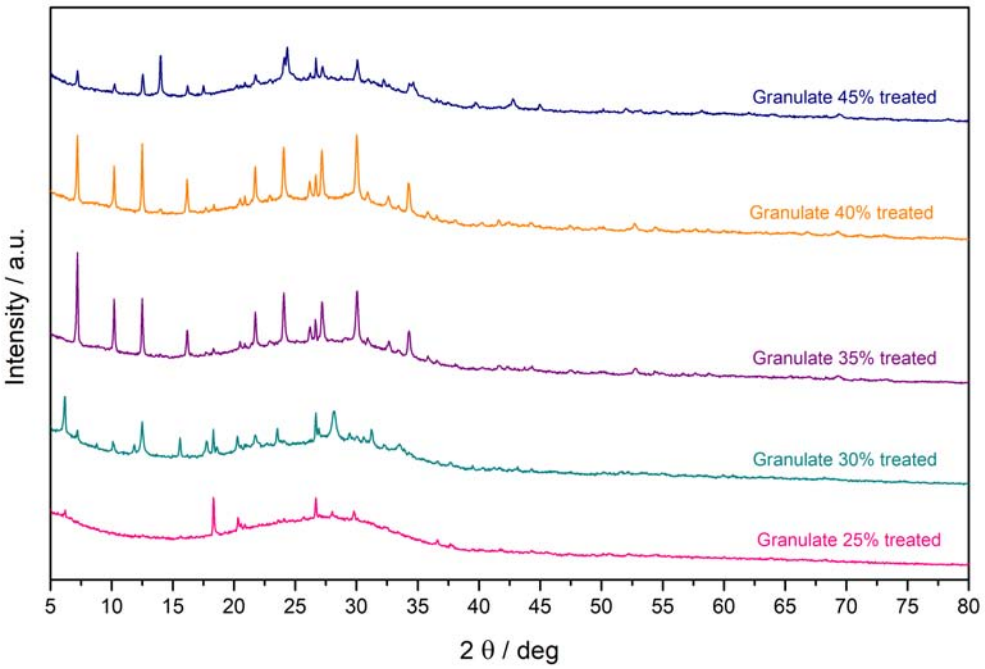

Figure 3.6: XRD conglomerate treated for each $NaAlO_2$ concentration

3.2 NMR analysis

The results derived by spectroscopy analysis XRD shows the presence of crystalline phase well defined within the binder. The more significant evidence of the formation of a semi-crystalline geopolymer-like alumino-silicate gel that surrounded unreacted soda-lime particles, came from the NMR spectroscopy. This analysis can be used to measuring the degree of reaction of the silica materials considering the evaluation of peak areas of Si NMR spectra, the intensity of each peak corresponds to the abundance of the Si-sites. High-resolution Si and Al NMR have proved to be a very technique for structural studies of silicates and aluminosilicates, for a deeper understanding of their structural properties as well as the process of formation[31].
One of the most important thing knows from NMR studies of silicate glasses [32] is that the connectivity of silicate networks is dependent on the amount of alkali present in the mixtures. For that reason, the analysis was conducted on the samples of binder with soda-lime powder both non-treated and treated, to understand the impact of treatment on the formation of the species.
Si NMR is capable to detect the SiO_4 tetrahedra connectivity ranging from 0 to 4, conventionally indicated by the symbol Q_m where the m corresponds to the bridging oxygen. This technique presents some problems when the spectra exhibit relatively broad peaks without observable separation. This might occur in the spectra of samples of Q_2, Q_3 and Q_4 corresponding to silicate tetrahedra and aluminum substituted silicate tetrahedra due to relatively small differences in chemical shift [49]. This shifts in aluminosilicate structures could be due to lower network connectivity and aluminum substitution in silicate units. The materials investigated do not consist on a structure made up of only a single type of Q unit. Typically, a geopolymer structure may present of various Q unit types of connected SiO_4 and AlO_4 tetrahedra depending on chemical composition. The Q units may be formed as Q_2 'chain or cycle like' structures, Q_3 'sheet like' and Q_4 'three dimensional' network.

Al NMR instead, provides information on different oxygen coordination around the Al atoms according to well-resolved peaks observed. With this

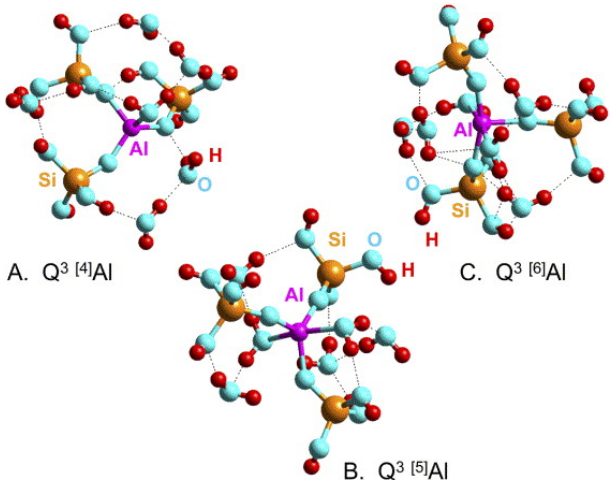

Figure 3.7: Four, five, six-fold coordinate Al ions

analysis could be evaluated the formation of AlO_4 tetrahedra typical of geopolymer structure. The signal around 55ppm occurs in the tetrahedral region of the ^{27}Al NMR chemical shift scale; it corresponds to a AlO_4 unit with silica as nearest neighbors and is typically observed in amorphous alumino-silicates and alumina-silica gels [52]. Six coordinate aluminum instead, with signal at 6 ppm, has the typical octahedral configuration. Figure 3.7 shows the alumino-silicate clusters with four, five and six-fold coordinate Al ions.

Figure 3.8 shows the ^{27}Al NMR spectra of the species with the main peaks around the value of 60ppm, consistent with the presence of Al ions in tetrahedral coordination (Al IV) like in conventional geopolymer [33]. The structure that results is a Si(IV)-O-Al(IV) network with the Na+ ions fundamental for the stabilization AlO_4 by charge compensation. In both samples there is minimal trace of characteristic peak of $NaAlO_2$ at 77-78 ppm (only a small shoulder), this proves that the sodium aluminate has dissolved and reacted virtually completely during curing [34]. The secondary peak in order to importance is around 74ppm corresponding to Al in five-fold coordination, both the samples presents that although with different intensity. The signal was weaker in the case of binder non treated which though is the only that presents a small intensity peak at 10ppm corresponding to six-fold coordinate Al ions. Therefore, the acid treatment favor the five-fold Al coordination to the detriment of six-fold. The main peak

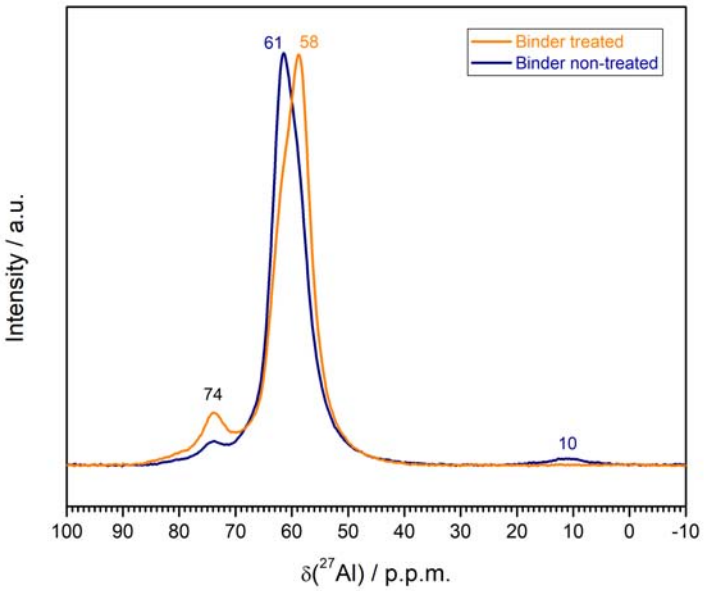

Figure 3.8: ^{27}Al NMR spectra

around 60ppm has some difference between glass powder treated and non-treated. The sample of soda-lime treated contained an enhanced ordering of AlO_4 units, considering the lower value of 58ppm, while the peak at 61ppm is typical of less ordered units.

The broad peaks in figure 3.9 in the range of -75ppm / -105ppm corresponds to the characteristic range of Q_4 species, with Q_4(mAl) sites with m=1,...,4. This resembles typical cementitious sodium aluminosilicate gels, which generally contain a distribution of Q_4(mAl) sites with m=1,. . . ,4 generally with the resonances of the Q_4(mAl) sites broadened so that their Si single-pulse MAS NMR spectra display only a similar broad hump [4]. The broad peak from Q_4 species derived from different Si-O-Al structures within the alumina-silicate gel. Signals at -84ppm, -91ppm, -96ppm and -102ppm are assigned silica units Q_4(4Al), Q_4(3Al), Q_4(2Al) and Q_4(1Al).
In the case of non treated sample prevails the Q_4(3Al) and Q_4(2Al), whereas Q_4(4Al) structures appear dominant in the sample of treated powder. In the spectra is possible to note a difference between the higher peaks of the treated and non treated curve. In particular, for the powder subjected by

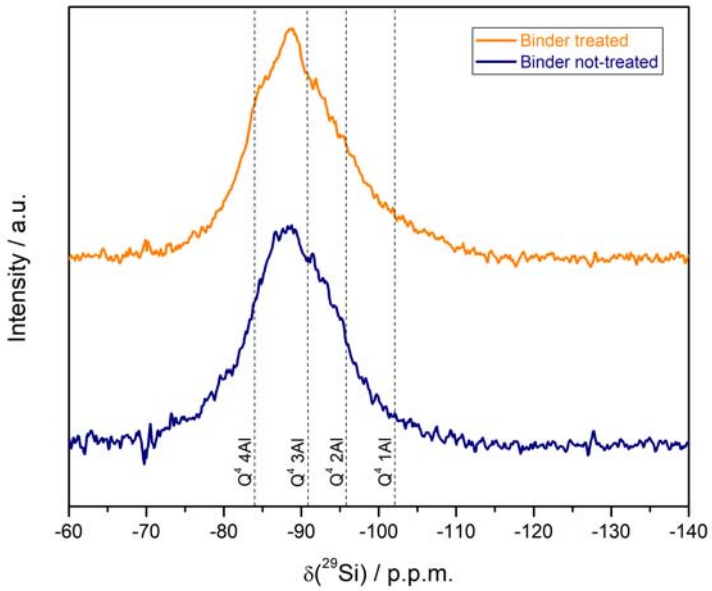

Figure 3.9: ^{29}Si NMR spectra

acid treatment, the main peak is at -89ppm correspond to the prevalent presence of Zeolite Na-A. Instead, the signal at 86ppm is consistent the presence of Hydrosodalite, which is dominant in the sample prepared from soda-lime powder non treated.

3.3 Morphological analysis

SEM analysis was conducted on specific samples to understanding the correlation between morphology and the concentration of activating solution. Moreover it was interesting comprehend the interface between binder and coarse glass particles in the fracture zone.
Two types of imagines were made during SEM analysis:

- BS backscattered electrons (elettroni radiodiffusi o elettroni di backscattering): backscattered electrons (BSEs) are high-energy electrons that are produced by the scattering of the incident electron beam with the atom nuclei. The trajectory of the electron from the primary beam that hits the surface of a sample, will be deviate by the interaction with the nuclei of the atoms. The ratio between the number of the emitted BSEs and the amount of primary beam, measured the yield of BSEs. This value depends on the atomic number, the higher is the atomic number or the heavier the element, the brighter the contrast. Typically, heavier elements with bigger nuclei, should deflect incident electrons more strongly than lighter elements. With this method, is it possible to evaluate the different constituting phases of the sample and density, however will be sacrifice the resolution and the tree-dimensionality of the image.

- ES secondary electrons: secondary electrons originate from the surface (or near-surface region) of the sample, are the result of inelastic interaction between the incident beam and test piece. This technique is useful to study the surface information of the sample, even if they are rough and roundish. The image that is obtained will be exceptionally tree dimensional.

The first impression at macroscopic level of the samples is of a massive materials, with good bonding with agglomerates putted in. The scan analysis was conducted on the polished surface and the fracture surface of each samples.

In the figure 3.10, which represents the fracture surface of conglomerate sample with 45% of activator, is possible to note how the binder surrounds

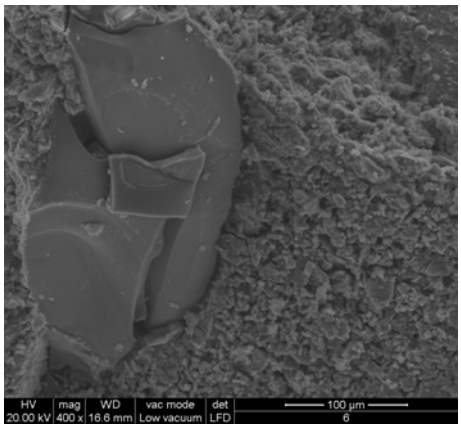

Figure 3.10: Conglomerate non-treated 45% $NaAlO_2$, fracture surface (400x-ES)

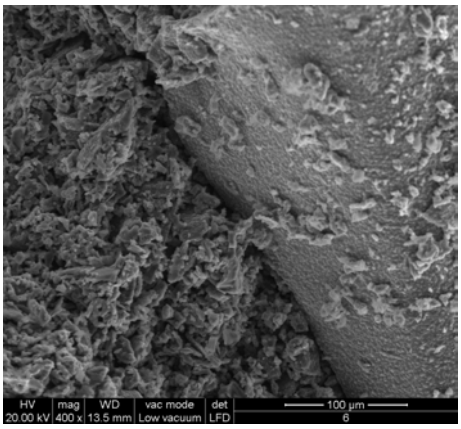

Figure 3.11: Conglomerate non-treated 25% $NaAlO_2$, fracture surface (400x-ES)

the glass coarse particle. The three-dimensionality of the secondary electrons image gives an idea of the fracture zone both for gel and for glass particle. At this level the geopolymer-like alumino-silicate gel results "spongy" and homogeneous, while the coarse particle has a typical glassy sharp fracture surface. It is evident that the fracture propagated mostly in the gel, but it could even pass across filler particles without pull-out phenomena. This is an important demonstration of the bonding energy of the interface between binder and coarse glass with the highest concentration of alkaline activator.

In the figure 3.11 show the interface between glass particle and binder with the lower concentration of activator (25% of $NaAlO_2$) in the fracture zone scan. Even for this sample the geopolymer like alumino-silicate gel results "spongy" and homogeneous, but the main difference respect figure 3.10 regards the aggregates morphology. In this case the coarse particle doesn't present a typical glassy sharp fracture surface, instead the filler remains intact with the outer part covered with residues of gel. This means that the binder isn't enough strong to hold the particles which show the pull-out phenomena. The fracture in this sample with lower concentration of activator, propagated in gel and in weak interface between binder and filler. The figure 3.12 shows the glass surface of the particle in the figure 3.11. In this image is possible to visualize zeolite crystals developed thanks to

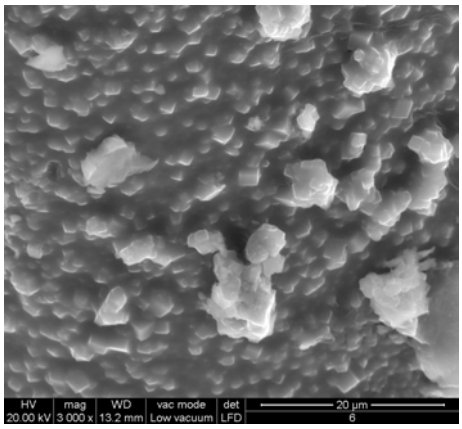

Figure 3.12: Conglomerate non-treated 25% $NaAlO_2$, fracture surface (3000x-ES)

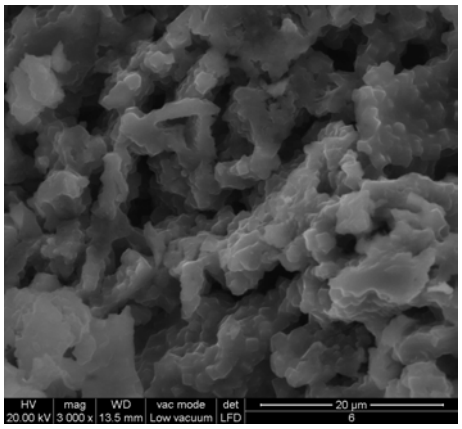

Figure 3.13: Conglomerate non-treated 25% $NaAlO_2$, fracture surface (3000x-ES matrix)

the reaction between the alkaline activator and the elements of the glass, in particular silica. Zeolitic phases are often not detected by SEM due to their occurrence in form of small crystals [35] or they present far from the perfect shape of pure zeolite [36]. However, as can be seen in figure 3.12, when the condition of growth are favorable, zeolites can be observed clearly. Zeolite Na-A exhibits forms as cubic crystal, well defined in the image. An energy dispersive X-Ray spectroscopy (figure 3.14, 3.15, 3.16) was conducted to analyzed the precise elements concentration in a particular zone of the surface. The data coming from the cubic crystals, confirm the presence of Si, Al, Na and Ca, attributable to zeolite that remains attached to the surface of glass particle even if occur the pull-out. Same analysis was conducted on another zeolitic crystal positioned far from aggregates (reported in figure 3.13), the results coming from the spectroscopy show that the stochiometric ratio between Si, Al, Na and Ca is almost the same respect to crystal attached to glass particle. The only difference in the graph regards the oxygen, this could be due to the different reaction of the glass powder during mixing respect to glass particles putted after the mixing.

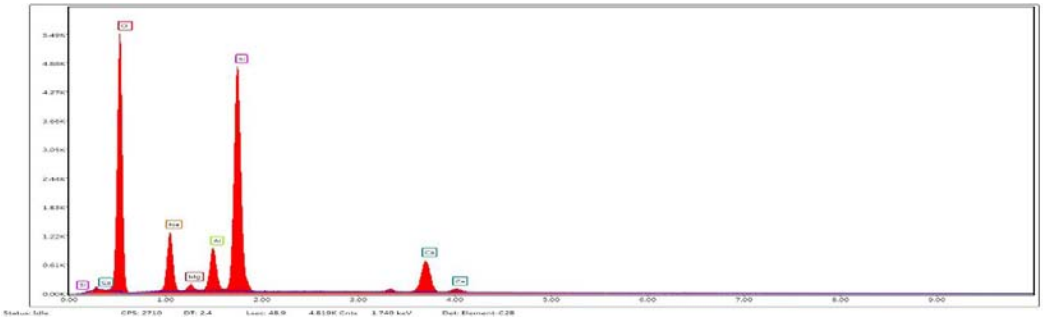

Figure 3.14: Energy dispersive X-Ray spectroscopy, conglomerate non-treated 25% $NaAlO_2$, fracture surface, Zeolite near the glass particle

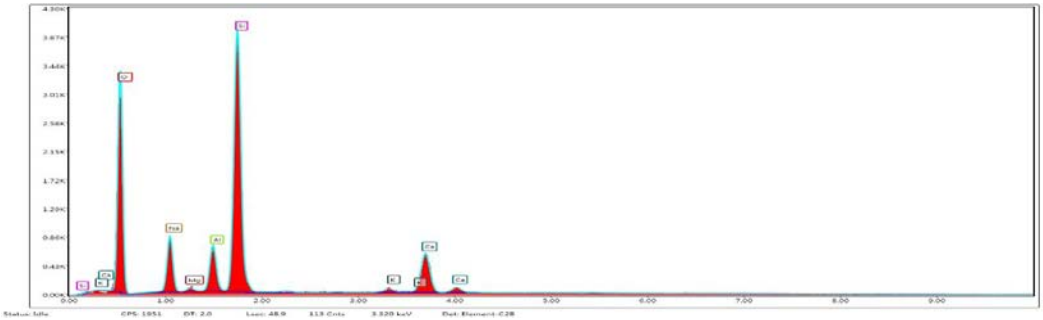

Figure 3.15: Energy dispersive X-Ray spectroscopy, conglomerate non-treated 25% $NaAlO_2$, fracture surface, Zeolite surrounded in the matrix

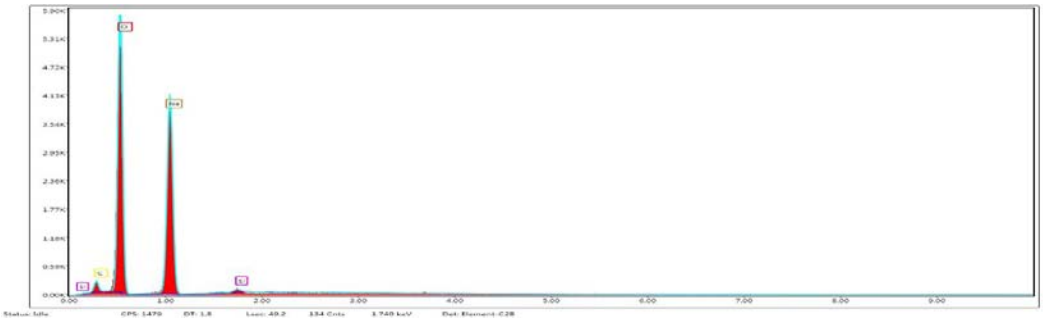

Figure 3.16: Energy dispersive X-Ray spectroscopy, conglomerate non-treated 45% $NaAlO_2$, efflorescence on polished surface

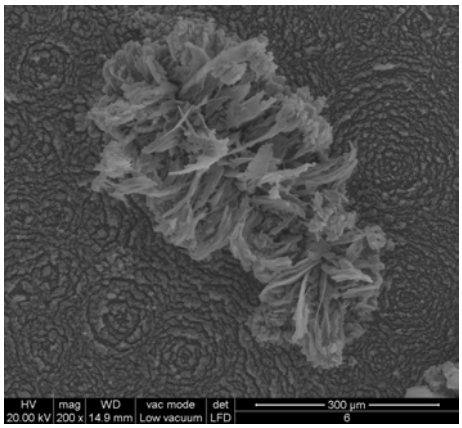

Figure 3.17: Conglomerate non-treated 45% $NaAlO_2$, polished surface (200x-ES)

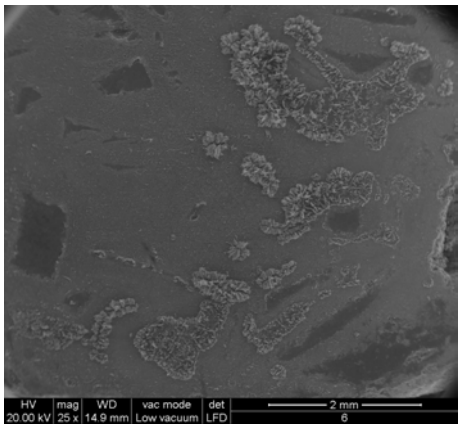

Figure 3.18: Conglomerate non-treated 45% $NaAlO_2$, polished surface (25x-ES)

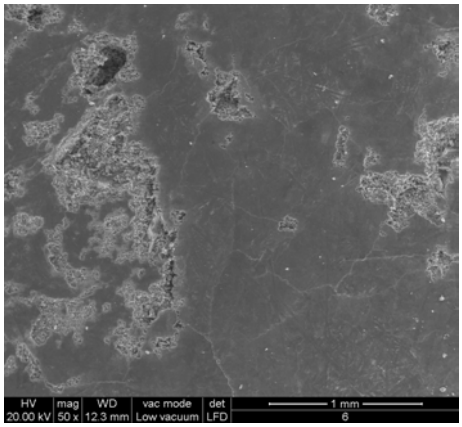

Figure 3.19: Conglomerate non-treated 25% $NaAlO_2$, polished surface (50x-ES)

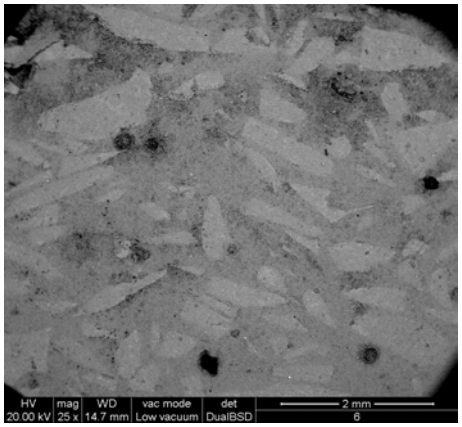

Figure 3.20: Conglomerate treated 45% $NaAlO_2$, polished surface (25x-BS)

Operating with as-received fine SLG powders, in the formulation of the matrix, resulted in efflorescence at the polished surface, shown in figure 3.17 and 3.18 according to energy dispersive X-ray spectroscopy (figure 3.16) the efflorescence corresponds to the formation of hydrated sodium carbonate, in turn consistent with the lower stabilization of alkali in the gel formed with not acid-treated glass powder. Sodium aluminosilicate geopolymers can suffer from un slightly efflorescence caused by excess sodium oxide remaining unreacted in the material. Sodium cations are mobile within the pore network, particularly when there is movement of moisture within the sample

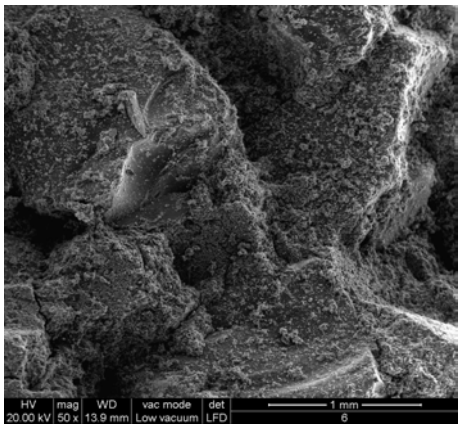

Figure 3.21: Conglomerate treated 45% $NaAlO_2$, polished surface (50x-ES)

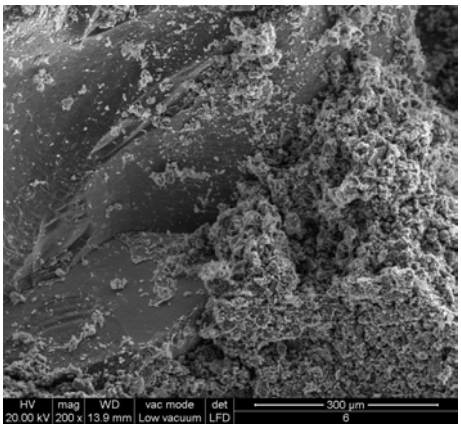

Figure 3.22: Conglomerate treated 45% $NaAlO_2$, polished surface (200x-ES)

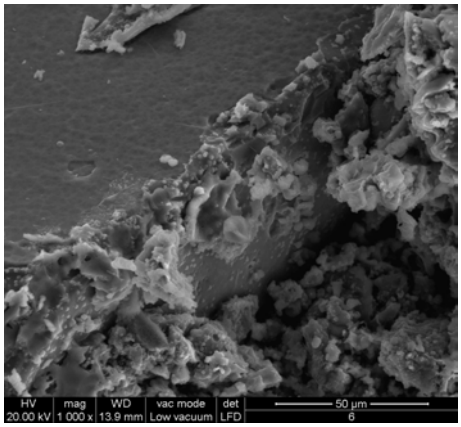

Figure 3.23: Conglomerate treated 45% $NaAlO_2$, polished surface (1000x-ES)

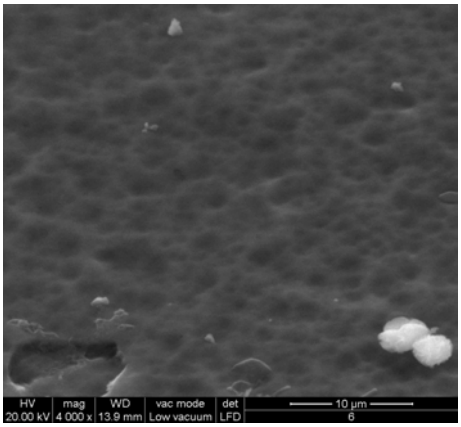

Figure 3.24: Conglomerate treated 45% $NaAlO_2$, polished surface (4000x-ES)

[37]. The tendency towards efflorescence in geopolymers is due partly to the very open microstructure of some materials which have a lower extent of reaction, partly due to the high alkali concentration in the pore solution [38] and also partly due to the relatively weak binding (and exchangeability) of Na in the geopolymer structure [39]. The alkalis can react with atmospheric CO_2, resulting in the formation of white layer of carbonate surface deposit, known as efflorescence.

This phenomena is distinct from the process of atmospheric carbonation of the binder that usually results in binder degradation, pH reduction and

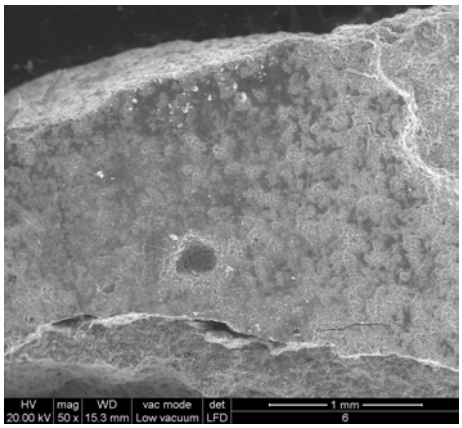

Figure 3.25: Binder non-treated 45% $NaAlO_2$, fracture surface (50x-ES)

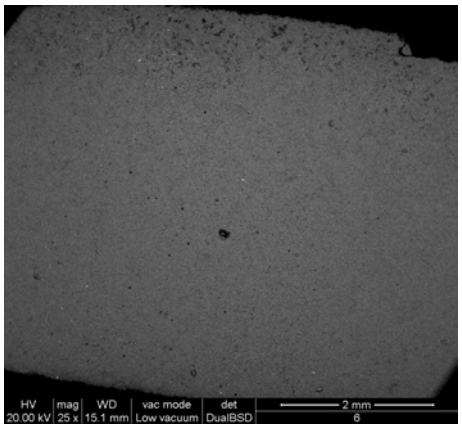

Figure 3.26: Binder non-treated 45% $NaAlO_2$, polished surface (25x-BS)

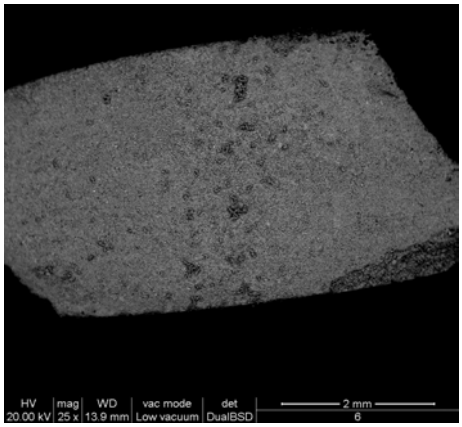

Figure 3.27: Binder treated 45% $NaAlO_2$, fracture surface (25x-BS)

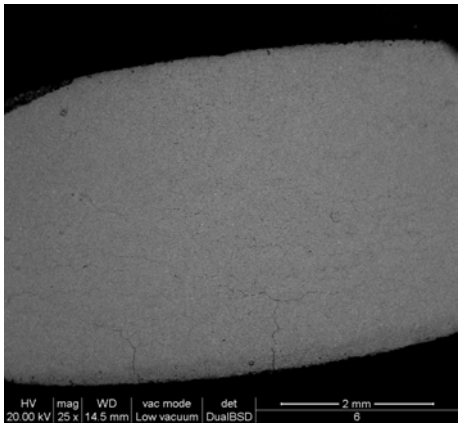

Figure 3.28: Binder treated 45% $NaAlO_2$, polished surface (25x-BS)

the deposition of carbonate reaction products in the sample, which may be visible to the naked eye. Efflorescence is different, they causes a formation of a thin deposit layer on the surface, and may or may not be accompanied by further degradation of the binder. Efflorescence is quite typical in geopolymers, and it may be prevented by introduction of additives (as an example, Provis and co-workers discussed the enhancement of alumina content in the gel, by addition of Ca aluminate or slag). For the geopolymeric binder derived from natural pozzolanic precursor for example, the presence of efflorescence can be reduced either by the addition of alumina-rich ad-

mixtures or by hydrothermal curing. Interestingly the surface of the sample with lower amount of alkaline activator (25% of $NaAlO_2$ in the solution) represented in figure 3.19, shows minor quantity of efflorescence. Instead, in the case of sample with glass powder treated binder, figure 3.20, there isn't any trace of efflorescence, so the acid treatment of the powder works. The figure 3.21 shows the fracture surface of the conglomerate sample with 25% of activating agent. Like in the case of the figure 3.11, the coarse particle doesn't present a typical glassy sharp fracture surface, instead the filler remains intact with the outer part covered with residues of gel. Cracks pass through the interface, but mostly remaining in the gel that hasn't sufficient bonding energy to hold the particles. The figure 3.23 allows to understand more closely the pull-out phenomena described before. In particular, it is possible to note the attack happened on the surface due to interaction with gel. Figure 3.24 shows more in detail the attached surface. It is interest to note the little white sphere in the corner, it has the shape, not so defined, of lamellar wool ball-like particles typical of Hydrosodalite.
The figure 3.25 and figure 3.27 represents the fracture zone of the sample with 45% of alkaline activator for soda-lime powder non treated, and soda-lime powder treated. The inner part of material is almost the same, the difference in treatment doesn't influence the homogeneity of the samples and without the presence of cracks. Even in the figures of polished surface 3.26 and 3.28 is possible to see the uniformity of the binder. It is interest to note that there aren't the presence of efflorescence in both of the samples.

3.4 Alkali mobility Test

The polymerization degree of alumino-silicate networks, in alumino-silicate glasses as well as in geopolymers, affects the mobility of alkali ions. In contact with distilled water, the specimens of the material release the alkalis bonded in the chain of tetrahedra Si-Al. Their presence in the water increase the pH of the water kept under control with litmus test. In our study were tested the samples with the lower concentration of activation agent (binder treated and non treated with 25% $NaAlO_2$) to understand the release of the less reticulated mixtures. The test was conducted with the binder sample with the lower concentration of alkaline activator ($NaAlO_2$), so the number of free alkali in the network is high compared to the 45% sample. To do this test, were taken 10g of material with dimension between 0,5mm and 2mm, for increase the surface contact with the water. The amount of distilled water necessary to completely cover the material was decided to be 30g. The test was started when the specimens were immersed in the water container.

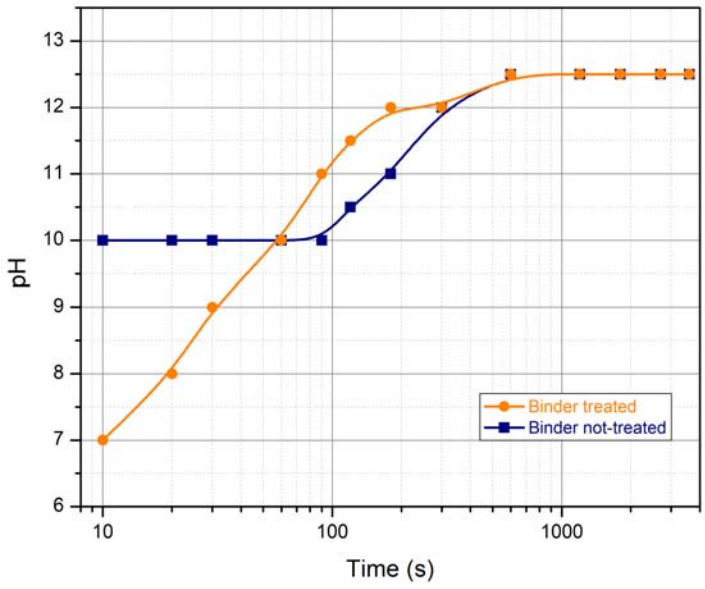

Figure 3.29: pH values

Time	0s	10s	20s	30s	60s	90s	120s	3m	5m	10m	20m	30m	45m	60m
binder non treated	6	10	10	10	10	10	10,5	11	12	12,5	12,5	12,5	12,5	12,5
binder treated	6	7	8	9	10	11	11,5	12	12	12,5	12,5	12,5	12,5	12,5

Table 3.3: pH values

With the collected data, it was possible to make some evaluation about the alkalis releasing. The substantial difference in the behavior between binder treated and non treated occur during the first 5 minutes. The increase of pH is more drastic for the binder non treated, with a change from 6 to 10 of the pH in the first 10s, instead for the binder treated the release is more gradual. The samples prepared from the pre-treated glass powder recorded a progressive increase of pH, from 7 to 12,5, within 10 minutes from the beginning of experiment. After 10 minutes the pH values settle down to the same value of 12,5 for each samples. That behavior is reasonable, since the alkali release is typical of geopolymer; anyway, the delay observed at the early stage of the immersion experiment can be considered as a further evidence of more polymerized gel, using acid-treated glass powder. The delay could be easily verified even by simple hand contact of bulk pieces: samples from pre-washed SLG were not 'slippery' as those from as-received SLG (in the latter samples, the sudden release of alkali likely induced saponification of epidermal fats).

3.5 Mechanical tests

Mechanical tests were conducted to evaluate the characteristic physical values of ours samples. Non-destructive and destructive tests were used to understand the differences on the behavior varying the composition and evaluate bonding strength between binder and filler particulate. In this section are presented the tests to calculate elastic modulus, compression strength, bending strength and an excursus on the theory of particulate composites. It's important to consider that the samples were tested for the mechanical properties seven months after their formation, so collected data could be consider the steady values of the materials [46].
Before the evaluation of mechanical strength is important to make come consideration about the conditions that influenced our samples. It's important to keep in mind those factors because for some data, particularly for strength properties, the results are strongly influenced by that.

- Microstructural strength: because Si–O–Si bonds are stronger than Si–O–Al and Al–O–Al bonds, it is expected that the strength of the activated mixtures will increase as the SiO_2/Al_2O_3 ratio increases [40]. Higher silica concentration lead the formation of Zeolite Na-A respect to Hydrosodalite, with the result of stronger bonding between the units. Based on results extract from XRD data, can be evaluate the crystalline phase of the samples understanding the relationship between phase concentration and mechanical characteristics.

- Degree of alkali reaction: the degree of reaction that determines the concentration of unreacted particles is important for the strength of network structure; glass powder not subjected to alkaline attack, doesn't dissolve their components which do not participate forming network structure. For those two factors, the concentration of alkaline activator ($NaAlO_2$) in the solution results fundamental [47].

- Samples dimension: another technical aspect is important for the confrontation with other construction materials: sample's dimension correlated to size of raw material. Mechanical test were conducted on element that have been made by cylindrical disk with height comprise

between 5mm and 8mm, and a diameter of 50mm. This samples have ratio between their dimension and raw material presents (in particular in the case of coarse glass particulate where the size are comprised between 300 μm to 1400 μm) infinitely higher respect to the test conducted on concrete tester made by ordinary Portland cement. In the case of compression and flexural tests for concrete materials, the samples are tapped directly in standard dimension mould. This modus operandi is different respect to our method where samples are machined before tests. Defects, inclusions, existing microcracks became more important influencing the values of the little samples.

- Samples preparation: the elements that were used to execute mechanical tests have been prepared previously with disk cutter and grinding with abrasives. This operation could lead the formation of microcracks in the samples, decreasing the mechanical properties of the virgin material.

- Porosity: porosity and pore size distribution influenced the microstructure of the material. In construction material, the excessive presence of pore caused reduction in mechanical strength and in elastic modulus. Some effects of pore-stress concentrations may occur due to tensile failure from a few or an isolated pore, or more general porosity under compressive loading [42]

3.5.1 Elastic modulus tests

For our study samples with similar dimension was taken (length = 40 mm, width = 5 mm, thick= 4 mm). The precise values of size of each samples are reported in table 3.4. The other characteristic data that was measured for each specimen was the mass, with which it was possible to evaluate the geometric density by considering the mass-to-volume ratio.
To measuring the characteristic frequency vibration, the sample was positioned in a two point base system with triangular supports, to minimize the interaction with the vibration of the bars. The sample is excited into vibration through the means of a light tap a vibrator detector is used to capture the vibrations, and to convert it into an electrical signal. The frequency detected by the device could corresponding to the horizontal and vertical longitudinal plane, this depend on how the impulse stress the section. Based on the repetition of the frequency revealed, it was selected the three main recurrent values attributable to the horizontal longitudinal plane.
From the graphs 3.30 and 3.31 is possible to evaluate the differences in terms of stiffness between binder and conglomerate for the non-treated solution.

The graph 3.30 shows the trend of elastic modulus in function of the

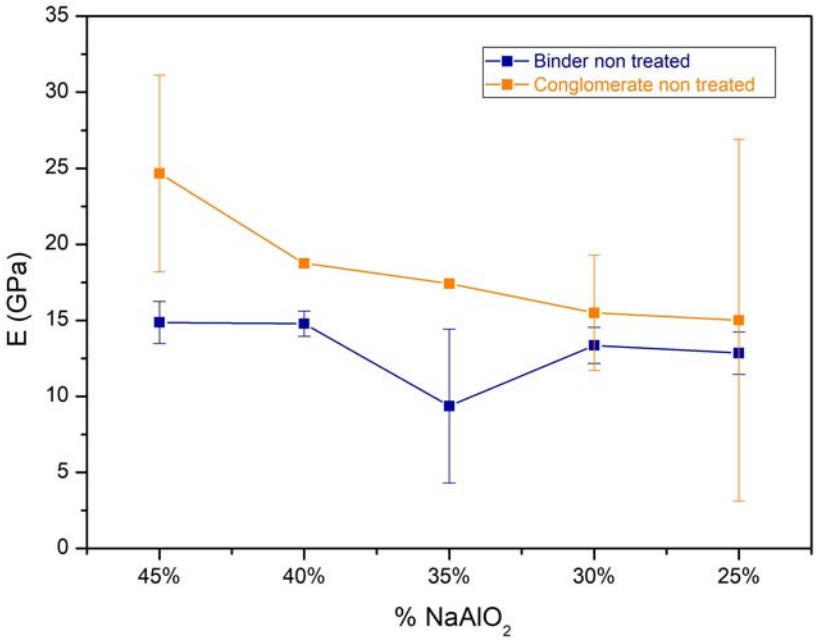

Figure 3.30: E / % $NaAlO_2$ samples not treated

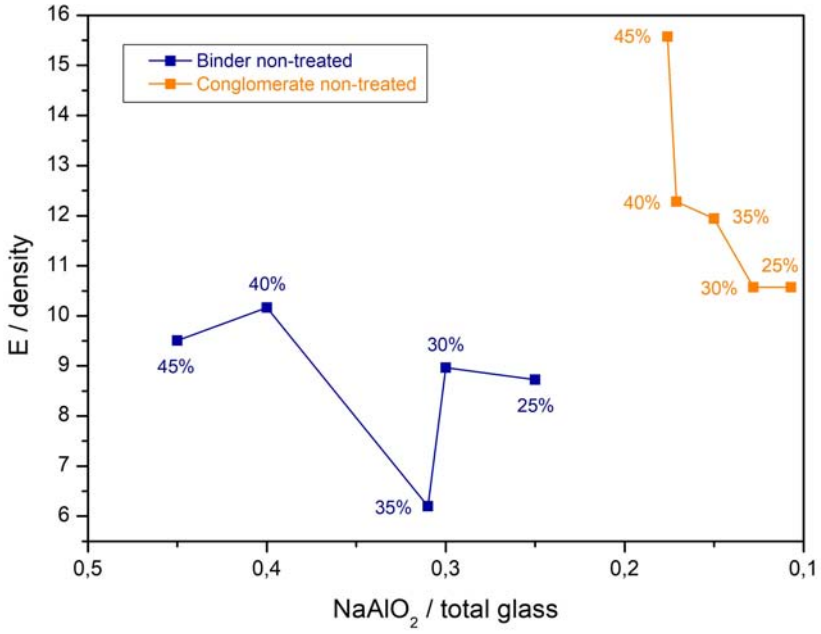

Figure 3.31: E rel / % $NaAlO_2$ rel samples non treated

$NaAlO_2$ percentage of the activating solution. Decreasing the amount of activating agent, the elasticity of the products reduces both for binder and for conglomerate. As expected form the theory of particulate composite, the addition of the glass particles increase the stiffness of the materials. The surface interaction between binder and agglomerate is sufficient to guarantee a good level of bonding in the material. In some cases is possible to see wide values of standard deviation, this means a considerable differences in the registered frequency. This can be evaluated as a consequence of the porosity of the material that influence the vibrational transmissions. The sample of binder with sodium aluminate percentage of 35% don't follow the decreasing trend of the other specimens, the reason could be the differences in the composition due to higher solid / liquid ratio as shown before in table 2.2.

The second graph in figure 3.31 describe the relation between the relative elastic modulus and the amount of sodium aluminate in function of the total glass of the sample. With this type of representation is possible to understand the importance of the addition of glass particles in the conglomerate specimens. Increasing the percentage of scrap (rough glass particles) al-

low to reduce the use of activating agent (unique wasteful raw material) to obtain the same mechanical performance of the binder. The decreasing trend is well defined for the conglomerate specimen, whereas for the binder samples still remain the problem with the piece with 35% of $NaAlO_2$. The lower position of 45% compared to 40% of sodium aluminate, is due to the higher density of the sample of 45% to the detriment of little increase of the elastic modulus, that reduce the position in the graph.

The graph 3.32 shows the same decreasing trend of the figure 3.30 but at lower values. Phases generated by acid treated powders results have weaker network bonding even if in those samples the amount of Zeolite Na-A is higher respect to samples non treated. Same behavior can be shows in figure 3.33 where the addition of filler particles decrease the ratio $NaAlO_2$ on total glass, but the performance remain almost the same of the relative binder. In this case there ins't a remarkable increase of the relative elastic modulus like for samples non treated; the reason could be the same of before, the weakness of the network bonding.

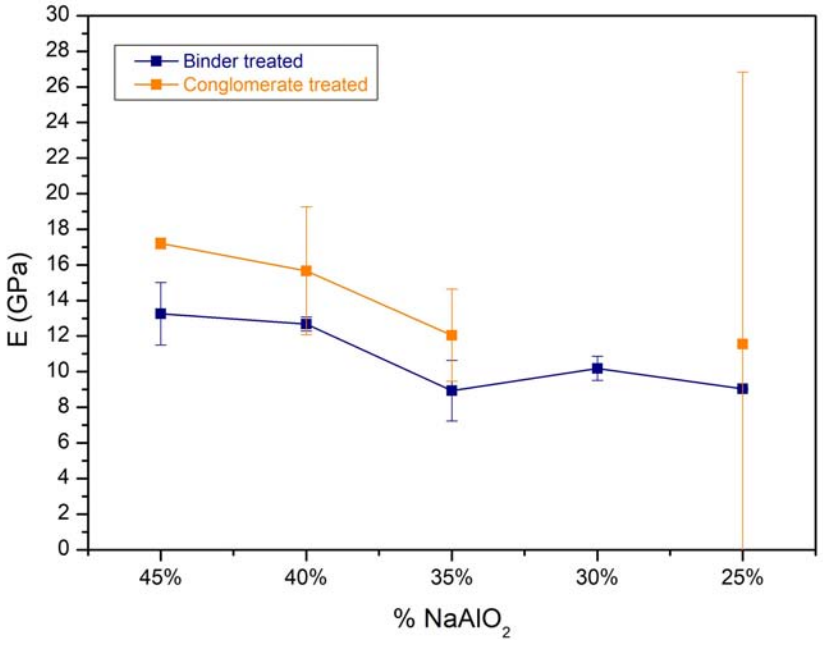

Figure 3.32: E / % $NaAlO_2$ samples treated

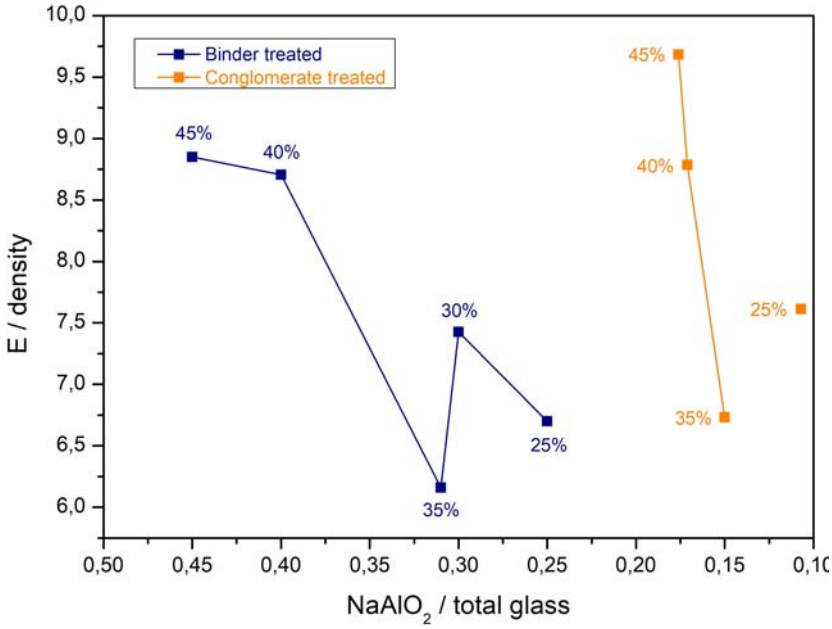

Figure 3.33: E rel / % $NaAlO_2$ samples rel treated

sample	% $NaAlO_2$	L (mm)	b (mm)	t (mm)	m (g)	f (Hz)	E (Gpa)	E / ρ
binder non treated	45%	43,7	5,2	4,1	1,457	6,59	14,87 ± 1,38	9,50
	40%	41,8	5	4	1,215	7,27	14,78 ± 0,83	10,17
	35%	42,3	7,9	4,7	2,373	6,30	9,33 ± 5,05	6,19
	30%	41,2	4,3	4,2	1,108	7,34	13,35 ± 1,18	8,96
	25%	42,3	4,6	4	1,145	6,57	12,84 ± 1,39	8,72
binder treated	45%	37,9	4,8	4,5	1,226	9,12	13,26 ± 1,76	8,85
	40%	40,7	5	4,1	1,215	7,25	12,68 ± 0,39	8,70
	35%	42,8	7,2	4	1,786	5,39	8,92 ± 1,70	6,15
	30%	40,8	4,7	4	1,052	6,51	10,18 ± 0,67	7,42
	25%	40,6	5,2	4,2	1,195	6,53	9,03 ± 0,06	6,69
conglomerate non treated	45%	40,5	6,7	4,3	2,08	9,59	24,66 ± 6,46	13,83
	45%	40,3	6,5	4,6	2,143	9,04	18,75 ± 0,21	10,54
	45%	40,6	6,8	4,3	2,027	8,24	17,42 ± 0,11	10,20
	45%	40,8	6,4	4,4	2,016	7,72	15,5 ± 3,80	8,83
	45%	40,3	6	4,6	1,889	7,88	15,01 ± 11,89	8,83
conglomerate treated	45%	40,6	6,9	4,8	2,39	8,91	17,21 ± 0,29	9,68
	45%	40,3	6,1	4,5	1,973	8,05	15,67 ± 3,59	8,78
	45%	44,2	7	4,4	2,437	5,78	12,05 ± 2,59	6,73
	45%	/	/	/	/	/	/	/
	45%	43,7	6,9	4,2	1,921	5,15	11,54 ± 15,29	7,61

Table 3.4: Elastic modulus results

Using CES Edupack software is possible to evaluate the performance of different materials on the basis of properties. In the case of Elastic modulus, it was added the range values obtained with the test to create the "cloud" for each material. Selection lines in the graph correspond to indices for beam (slope = 2) and for pannel (slope = 3).

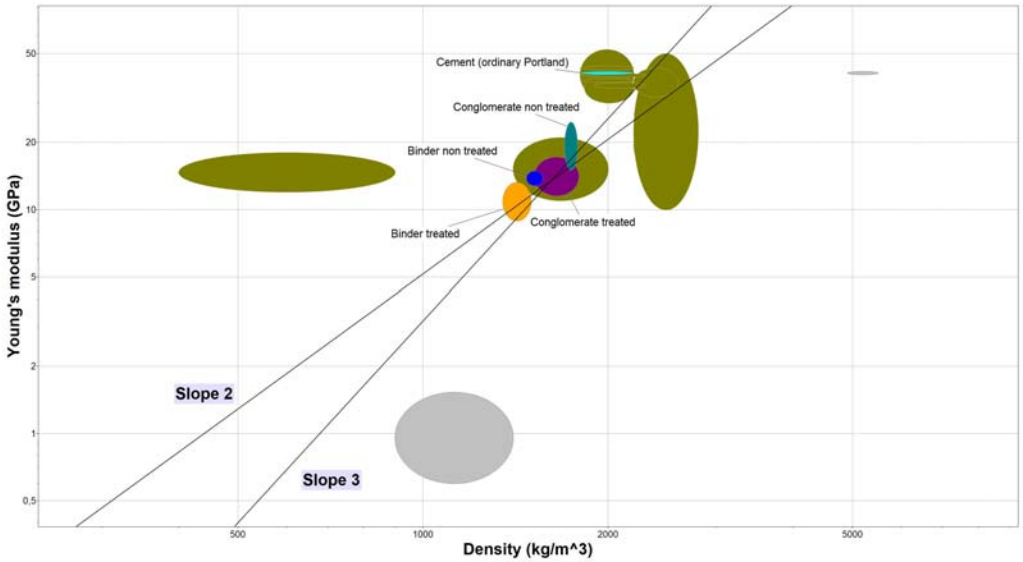

Figure 3.34: Ashby diagram for Elastic modulus / Density

3.5.2 Compression tests

For compression test, the ideal curve in load/deformation graph was structured with an initial high slope until the maximum load value, and a slow descent due to minor resistance exhibit by the breaked sample. In some cases is possible to see local maximum in the first part of the test because of partial breakage of the sample.
Mechanical properties, and in particular compressive strength, are influenced by the transformation of amorphous gel into zeolites causes the reorganization of local structure. It can be assumed that there is a certain limit of zeolite content that can be support by a geopolymeric matrix, after which it causes its weakening [4]. This weakening may be the results of bonding strength, or zeolite crystalline phases may act as a defect within the geopolymer matrix. Another factor that influence the reduction of compressive strength gives by zeolites are their microporous-crystalline structure based on 3D-cage system when compared to the amorphous structure constitute by silica and aluminum tetrahedra.
Our tests were conducted on cubic samples with approximately standard dimension: 5 mm height with 7 mm x 7 mm for the base. For every concentration were prepared three samples to obtain a degree of approximation that eliminate the variability caused by the defects within the bulk. Before the destructive test, it was measured the surface contact of the pieces in order to calculate the compressive strength with the general compression equation. With the machine was calculated the maximum value of the force until the breakage.
In the table 3.5 are collected the data for each concentration. The indicated σ_{comp} is an average value of each sigma calculated by the sample.

The graph 3.35 show the trend for each types of samples in decreasing concentration. The results are in line with the expectation: with lower concentration of alkaline solution, the strength of the materials is reduced. Even if the amount of Zeolite Na-A is higher in samples with lower concentration of $NaAlO_2$ (Zeolite with higher bonding force), the strength results higher for species with major alkaline activator. Those results were verified for all the types of species, binder/conglomerate and non-treated/treated. Respect to Young modulus, in this case the binder show higher value of

sample	$\%NaAlO_2$	σ_{comp} (MPa)	sample	$\%NaAlO_2$	σ_{comp} (MPa)
binder non treated	45%	49,04 ± 7,27	conglomerate non treated	45%	19,53 ± 0,71
	40%	43,67 ± 5,58		40%	18,91 ± 6,31
	35%	39,22 ± 5,83		35%	14,19 ± 8,25
	30%	36,64 ± 1,00		30%	12,68 ± 5,88
	25%	35,43 ± 4,91		25%	6,54 ± 2,40
binder treated	45%	39,09 ± 2,12	conglomerate treated	45%	20,29 ± 3,10
	40%	36,91 ± 6,71		40%	20,51 ± 1,93
	35%	23,75 ± 4,38		35%	13,01 ± 2,58
	30%	18,80 ± 10,87		30%	/
	25%	12,78 ± 4,59		25%	2,68 ± 0,31

Table 3.5: Compression tests results

strength, this could be demonstrate by the fact that, even if the glass filler has good bond with geopolymeric/zeolitic matrix, they favored the crack propagation by weak bonding in the interface. The reinforce given by the particles lead to an increase in the performance in terms of elastic modulus, but not for compressive strength. Increasing the amount of glass (glass particulate) added to the synthesis mixtures lead to a decrease in the compressive strength of the activated mixture. This behavior was attributed to

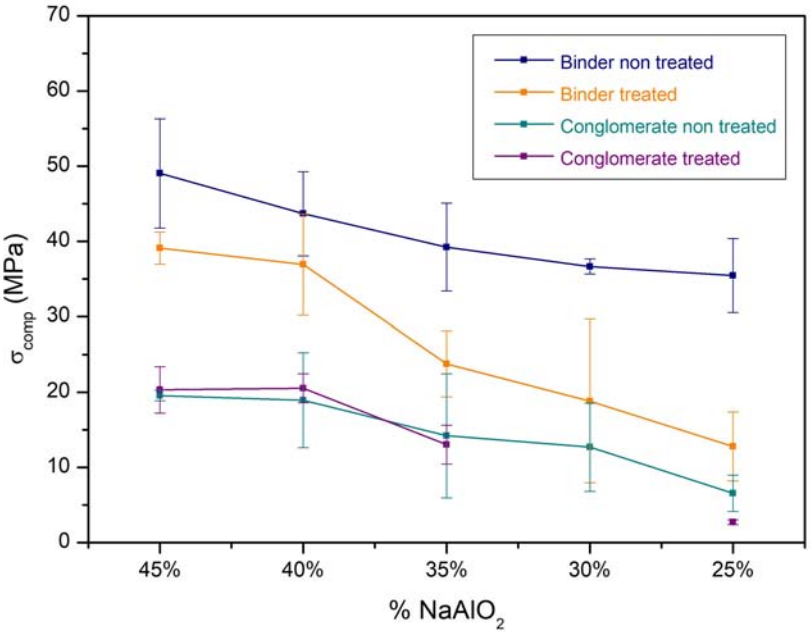

Figure 3.35: Compression strength / % $NaAlO_2$

changes in the microstructure of the activated mixture due to an increase in overall SiO_2/Al_2O_3 molar ratio upon waste glass addition [2].
Using CES Edupack software is possible to evaluate the performance of different materials on the basis of properties. In the case of compression strength, it was added the range values obtained with the test to create the "cloud" for each material. Selection line in the graph correspond to indices of compression (slope =1)

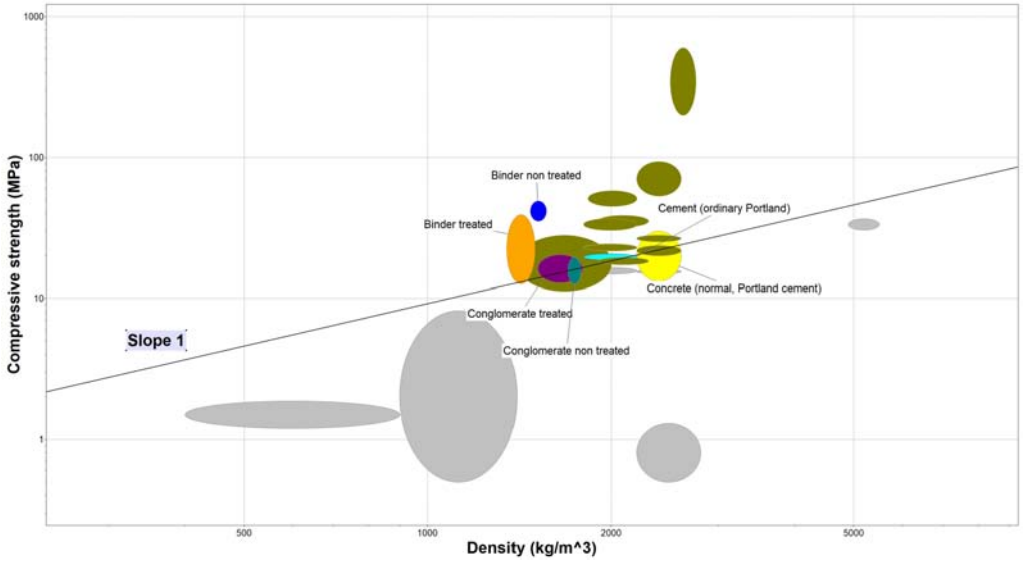

Figure 3.36: Ashby diagram for Compressive strength / Density

3.5.3 Three-point flexural test

The examination of flexural strength is one of the widespread test carried out on hardened concrete that confirm the load at which the crack propagates in the element. The samples were prepared with similar dimension: 5 mm height, 6/7 mm wide and 40 mm length. For each concentration was executed nine tests on different samples to obtain the values of force needed to break the pieces.
The load curves demonstrate a linear behavior until the fracture is fragile following an abrupt drop when the strength of the fracture is attained. Different slopes of the linear part reflect the different values in Young's module, even though influenced by the actual cross section of the samples.

The figure 3.37 display the trend of the average modulus of rupture of the specimens at varying of the concentration of alkaline activator. For this test the results are not clearly like for the compression strength, with the initial consideration of the chapter that become more relevant in this case . The type of fracture suffered the presence of micro-cracks and unreacted/aggregate particles that acts as localized stress concentration. Therefore, the values are influenced by the quality of the samples used for the test.

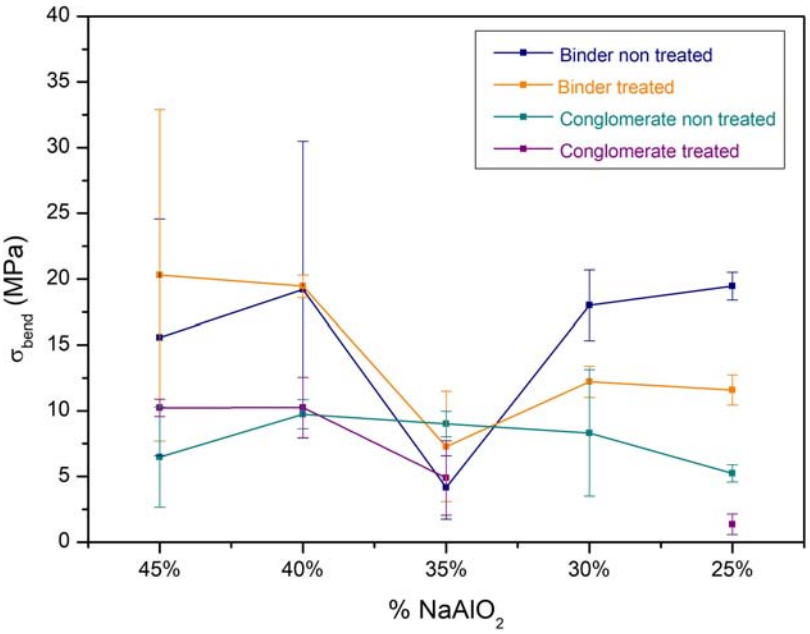

Figure 3.37: Bending strength / % $NaAlO_2$

In case of 35%, the difference in solid / liquid ratio influence the geopolymerization reaction with the bending strength values that don't follow the linear course. For specimens of binder treated the trend is almost linear with decreasing of concentration, with only exception of 35%. Modulus of rupture are in the range between 20 MPa and 10MPa with major value for the species with higher degree of activation. Binder non-treated show a trend not so reliable, excluding the 35% result, the range is between 20MPa and 15MPa, with lower concentration that exhibit similar values of bending strength of the samples with higher alkaline activator. For the binder, the results show that the acid treatment influence the bending properties of the samples, the network structures are weaker than binder non treated for lower activator concentration, whereas are stronger for major concentration. The major amount of Zeolite Na-A for minor concentration of $NaAlO_2$ in this case shows their effect. Same trend, but for lower values, is possible to see for the conglomerate samples. In this case the presence of 40% volume fraction of glass particulates strongly decrease the mechanical properties respect to the binder. The values of bending strength are comprised in the range of 10MPa and 5MPa, with the exception of 30% and 25% for treated conglomerate.
In table 3.6 were presented the data coming from the calculation described in section 2.4.3.

sample	$\%NaAlO_2$	σ_{bend} (MPa)	sample	$\%NaAlO_2$	σ_{bend} (MPa)
binder non treated	45%	15,56 ± 8,98	conglomerate non treated	45%	6,47 ± 3,81
	40%	19,21 ± 11,27		40%	9,74 ± 1,10
	35%	4,16 ± 2,40		35%	9,01 ± 0,97
	30%	18,01 ± 2,67		30%	8,31 ± 4,81
	25%	19,45 ± 1,05		25%	5,23 ± 0,65
binder treated	45%	20,29 ± 12,59	conglomerate treated	45%	10,22 ± 0,65
	40%	19,45 ± 0,85		40%	10,25 ± 2,30
	35%	7,28 ± 4,20		35%	4,88 ± 2,83
	30%	12,21 ± 1,18		30%	/
	25%	11,58 ± 1,13		25%	1,36 ± 0,78

Table 3.6: three-point flexural tests results

Using CES Edupack software is possible to evaluate the performance of different materials on the basis of properties. In the case of bending strength, it was added the range values obtained with the test to create the "cloud" for each material. Selection line in the graph correspond to indices of bending for beam (slope = 1,5) and pannel (slope = 2)

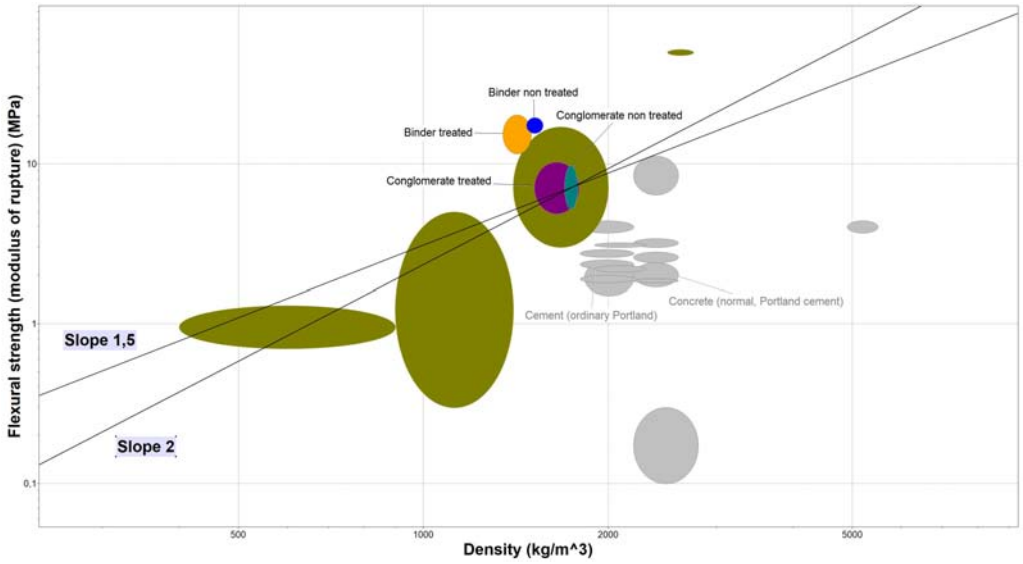

Figure 3.38: Ashby diagram for Bending strength / Density

3.5.4 Porosity evaluation

The material's porosity arises from mesoporous nature of the geopolymeric gel, unreacted soda-lime powder or entrapped air remain in the sample. All specimens show high densities and low porosity, approximately 25 % / 35%, in agreement with other similar materials found in literature.
Porosity and pore size distribution are vital components of the microstructure of cement paste. Pore structure influenced the permeability of cement and thus the extent of penetration by aggressive agents. The presence of zeolites in a geopolymeric matrix affects bulk density and apparent porosity. Typically, the values of porosity and pore volume increases in such composites when compared to geopolymers without zeolites [4]. Generally, increase in water content, gives major porosity to the structure.

In table 3.7 is it possible to see the trend of the porosity with decreasing concentration. Low alkaline activator leads to highest total porosity as a result of poor reaction of the initial materials and lack of cohesion between the unreacted particles, as the geopolymeric gel is not produced in sufficient extension. This phenomena is better defined for binder with treated powder, respect to binder non treated, with the total porosity that increase from 33,32% for 45% of $NaAlO_2$ to 38,14% for 25% of $NaAlO_2$.
The increase in SiO_2/Al_2O_3 ratio that could be seen as an indicator of en-

sample	$\%NaAlO_2$	$\rho_{geom}(g/cm^3)$	$\rho_{app}(g/cm^3)$	$\rho_{true}(g/cm^3)$	$\Phi_{open}(\%)$	$\Phi_{clos}(\%)$	$\Phi_{tot}(\%)$
binder non treated	45%	1,564	2,165	2,213	27,78	1,56	29,34
	40%	1,453	2,158	2,205	32,65	1,45	34,10
	35%	1,510	2,164	2,224	30,17	1,88	32,06
	30%	1,489	2,197	2,243	32,21	1,38	33,60
	25%	1,472	2,138	2,196	31,15	1,80	32,96
binder treated	45%	1,498	2,193	2,247	31,68	1,64	33,32
	40%	1,456	2,219	2,227	34,36	0,24	34,60
	35%	1,449	2,212	2,217	34,49	0,12	34,62
	30%	1,371	2,120	2,204	35,31	2,48	37,79
	25%	1,347	2,141	2,179	37,06	1,07	38,14
conglomerate non treated	45%	1,782	2,329	2,376	23,47	1,50	24,97
	40%	1,778	2,319	2,341	23,32	0,69	24,02
	35%	1,707	2,331	2,359	26,73	0,88	27,62
	30%	1,755	2,332	2,357	24,73	0,79	25,53
	25%	1,698	2,349	2,353	27,69	0,12	27,81
conglomerate treated	45%	1,777	2,349	2,358	24,35	0,30	24,65
	40%	1,784	2,326	2,359	23,31	1,05	24,37
	35%	1,790	2,332	2,333	23,25	0,01	23,27
	30%	/	/	/	/	/	/
	25%	1,516	2,339	2,352	35,18	0,35	35,53

Table 3.7: Porosity calculation results

hanced properties, produced a decrease in total porosity.
Important difference in terms of closed porosity are not registered. Respect to the variation of composition, the material has a limited percentage of closed porosity which still remain almost 1%. Major differences between the samples regards the open porosity, for which become important the composition of the mixture: amount of alkaline activator and therefore the SiO_2/Al_2O_3 ratio.

3.5.5 Particulate composites

Addition of rigid particles to glass matrix can produce a number of desirable effects; for example an increase in stiffness, a reduction in the coefficient of thermal expansion and an improvement in creep resistance and fracture toughness [41]. The final behavior of the material results from a complex interplay between the properties of the individual constitute phases: the binder, the agglomerate and the interface. For particulate composite the model to estimate the elastic modulus of the material derives from the constituent equation, where the values of matrix and reinforce are in relation with the volume fraction of the reinforce.

$$E_{comp} = \frac{E_p \cdot E_m}{E_p \cdot V_m + E_m \cdot V_p} \tag{3.1}$$

where:

- E_{comp} is the elastic modulus of the conglomerate
- E_m is the elastic modulus of the matrix
- E_p is the elastic modulus of the filler particles
- V_m is the volume fraction of the matrix
- V_p is the colume fraction of the filler particles

The equation corresponds to the lower curve of the elastic modulus/volume fraction graph 3.39, but in the case of conglomerate with heterogeneous particles is obtained a good value of elasticity due to the high volume fraction of the reinforcement. The solution given by equation assume that the individual phases are under uniform strain or stress, respectively. In practice, however, the filler particles may not be completely separated from one another and the reinforcement element may effectively be an aggregate of smaller particles on the microlevel. Thus in response to the applied load the stress will be distributed unevenly between the particles and aggregates, and the assumption of either uniform stress or uniform strain is clearly an oversimplification. The theory which explain the reinforcing action of a filler assume perfect adhesion between the filler and the binder. In the case of

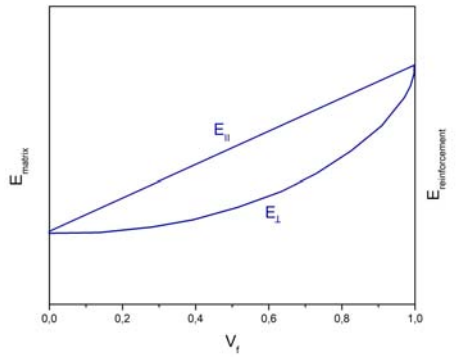

Figure 3.39: elastic modulus / reinforcement volume fraction

imperfect adhesion, the non-bonded particles acted as holes, and therefore, predicted a decrease in modulus with increasing filler content. In our study was tested the feasibility of the glass particle addition and how they interacted with the glass binder. Subsequent researches may concern the packing density of the particles in function of their dimension and the wettability of the matrix. Mixtures of particles with differing size can pack more densely than monodispersed particles because the small ones can fill the interstitial space between the closely packed large particles to form an agglomerate.

Chapter 4

Conclusion

In this work, alkaline activated geopolymer-zeolite material principally constituted by soda-lime glass waste, has been characterized and tested. Two types of raw materials were used, common glass powder and acid treated glass powder, to understand the influence of alkali in geopolymerization reaction. Focus has been given on the composition of the mixture, in particular decreasing the concentration of sodium aluminate in activating solution. The influence of the composition was evaluated characterizing the microstrucure of the samples, analyzing them with mechanical test to understand the performance of the materials.
The alkali-activated materials produced by reaction between alkaline solution and solid aluminosilicates, are also known as Geopolymeric cements, are becoming more important in construction field for in view of a lower enviromental impact. Respect to the previous solution, ours geopolymer-zeolite samples were realized using almost totally waste coarse glass, demonstrating the feasibility of a project that has as object the maximum valorization of recycled material.
The obtained results and observation are summarized below.

- Concentration of sodium aluminate as alkaline activator represents one of the main factors that influenced the materials. Decreasing the amount in the activating solution, the quality of the samples in terms of networks structure, bonding strength and mechanical properties is reduced.

- The ratio between solid and liquid influences the geopolymerization reaction allowing the phenomena of dissolution and polycondensation between the species of the blend. A system where the solid to liquid ratio is 50 / 50 allows to obtain the best results.

- The proportion between silica and alumina governs the possibility of formation of zeolitic phase, and their types, during geopolymersization. The kind of zeolites present in the geopolymer-zeolite material strictly depends on the composition of the gel from which they crystallize.

- Differences between types of raw materials used are well defined in the microstructural and morphological analysis (XRD, NMR, SEM). Instead, mechanical tests have shown small difference in terms of performance, with non treated samples that have better compressive strength and elastic modulus.

- The addition of coarse glass particle as aggregates in the blend binder, don't influence geopolymerization reaction. The obtained conglomerate material features better elastic modulus respect to their binder (matrix) as expected by the particulate composite theory. Moreover, it is possible to increase the fraction, even of different types, of waste glass contained in mixtures.

Bibliography

[1] R. V Silva, J. De Brito, C. Q. Lye, and R. K. Dhir, *The role of glass waste in the production of ceramic-based products and other applications : A review*, J. Clean. Prod., vol. 167, pp. 346–364, 2017

[2] M. Waguchi, T. Kato, Y. Imamura, N. Yoshida, and S. Aoki, *Challenge to improve glass melting and fining process*, Ceram. - Silikaty, vol. 52, no. 4, pp. 218–224, 2008

[3] J. Escalante-Garcia, *Overview of potential of urban waste glass as a cementitious material in alternative chemically activated binders*, J. Chin. Ceram. Soc. 43 (2015) 1441–1448. 10. 14062/j.issn.0454-5648.201 5.10.14

[4] G. Kastiukas, X. Zhou, J. Castro-Gomes, *Development and optimisation of phase change material-impregnated lightweight aggregates for geopolymer composites made from aluminosilicate rich mud and milled glass powder*, Constr. Build. Mater. 110 (2016) 201–210

[5] J. L. Provis, S. Bernal, *Geopolymers and related alkali-activated materials*, Annu. Rev. Mater. Res. 2014. 44:299–327

[6] P. Duxson, A. Fernández-Jiménez, J.L. Provis, G.C. Lukey, A. Palomo, J. Van Deventer, *Geopolymer technology: the current state of the art*, J. Mater. Sci. 42 (2007) 2917–2933

[7] J. Vrijders, J. Desmyter, *Stimulate a High Use of Puing Granules*, OVAM, Mechelen, 2008

[8] L. K. Turner, F. G. Collins, *Carbon dioxide equivalent ($CO_2 - e$) emissions: A comparison between geopolymer and OPC cement concrete*, Construction and Building Materials 43 (2013) 125–130

[9] P. Rozek, M. Krol, W. Mozgawa, *Geopolymer-zeolite composites: A review*, Journal of Cleaner Production 230 (2019) 557e579

[10] A. Buchwald, H.D. Zellmann, C. Kaps, *Condensation of aluminosilicate gelsmodel system for geopolymer binders*, Non-Cryst. Solids 357, 1376e1382

[11] R.H. Kupaei, U.J. Alengaram, M.Z. Jumaat, *The effect of different parameters on the development of compressive strength of oil palm shell geopolymer concrete*, Sci. World J. 2014 (2014) 898536.

[12] P. Duxson, J. L. Provis, G. C. Lukey, S. W. Mallicoat, W. M. Kriven, J. S. J. Van Deventer, *Understanding the relationship between geopolymer composition, microstructure and mechanical properties*, Colloids and Surfaces A: Physicochem. Eng. Aspects 269 (2005) 47–58

[13] E.D. Rodríguez, S.A. Bernal, J.L. Provis, J. Paya, J.M. Monzo, M.V. Borrachero, *Effect of nanosilica-based activators on the performance of an alkali-activated fly ash binder*, Cement Concr. Compos. 35, 1e11

[14] Z.H. Liu, Q. Tang, C.M. Li, Y. He, X.M. Cui, *Preparation of NaA zeolite spheres from geopolymer gels using a one-step method in silicone oil*, Int. J. Appl. Ceram. Technol. 14, 982e986

[15] P. Sturm, S. Greiser, G. J. G. Gluth, C. Jager, H. J. H. Brouwers, *Degree of reaction and phase content of silica-based one-part geopolymers investigated using chemical and NMR spectroscopic methods*, J Mater Sci (2015) 50:6768–6778

[16] J. Davidovits, *Geopolymer Chemistry and Applications, 3rd Edition*, Geopolymer Institute, 2011

[17] P. Duxson,G.C. Lukey, F. Separovic, J. S. J. van Deventer, *Effect of alkali cations on aluminum incorporation in geopolymeric gels*, Ind Eng Chem Res 2005;44(4):832–9

[18] A. Hajimohammadi, J. L. Provis, J. S. J. Van Deventer, *One-Part Geopolymer Mixes from Geothermal Silica and Sodium Aluminate*, Ind. Eng. Chem. Res. 2008, 47, 9396–9405

[19] N. Granizo, A. Palomo,A. Fernandez-Jimenez, *Effect of temperature and alkaline concentration on metakaolin leaching kinetics*, Ceram. Int. 40, 8975e8985

[20] P. Duxson, A. Fernandez-Jimenez, J. L. Provis, G. C. Lukey, A. Palomo, J. S. J. van Deventer, *Geopolymer Technology: the current state of art, Advances in geopolymer science and technology*, J Mater Sci (2007) 42:2917–2933, DOI 10.1007/s10853-006-0637-z

[21] N. Nordin, M.M.A.B. Abdullah, M.F.M. Tahir, A.V. Sandu, K. Hussin, *Utilization of fly ash waste as construction material*, Int. J. Conserv. Sci. 7 (2016)

[22] N. Toniolo, A. Rincón, J.A. Roether, P. Ercole, E. Bernardo, A.R. Boccaccini, *Extensive reuse of soda-lime waste glass in fly ash-based geopolymers*, Construction and Building Materials 188 (2018) 1077–1084

[23] F. Puertas, M. Torres-Carrasco, *Use of glass waste as an activator in the preparation of alkali-activated slag. Mechanical strength and paste characterisation*, Cem. Concr. Res. 57 (2014) 95–104

[24] J. Davidovits, *Properties of Geopolymers cements*, Geopolymer Institute, 02100 SAINT-QUENTIN – France

[25] T. Luukkonen, Z. Abdollahnejad, J. Yliniemi, P. Kinnunen, and M. Illikainen, *One-part alkali-activated materials: A review*, Cem. Concr. Res., vol. 103, no. July 2017, pp. 21–34, 2018

[26] R. Hemmings and E. Berry, *On the glass in coal fly ashes: recent advances*, in MRS Proceedings, Cambridge University Press, 1987, p. 3.

[27] M. M. Selim, D. M. EL-Mekkawi, R. M.M. Aboelenin, S. A. Sayed Ahmed, G. M. Mohamed, *Preparation and characterization of Na-A zeolite from aluminum scrub and commercial sodium silicate for the removal of Cd2+ from water*, Journal of the Association of Arab Universities for Basic and Applied Sciences (2017) 24, 19–25

[28] A. Gualtieri, P. Norby, G. Artioli, J. Hanson, *Kinetics of formation of zeolite Na-A (LTA) from natural kaolinites*, Phys Chem Minerals (1997) 24: 191–199

[29] B. C. Bunker, T. J. Headley, and S. C. Douglas, *Gel Structures in Leached Alkali Silicate Glass*, MRS Proc., vol. 32, p. 41, 1984

[30] S. Greiser, G. J. G. Gluth, *RSC Advances aluminosilicate gels (geopolymers) and gel – zeolite composites*, pp. 40164–40171, 2018

[31] G. Engelhardt, D. Michel, *High-Resolution solid-state NMR of silicates and Zeolites*, John Wiley & Sons Ltd., 1987

[32] P. S. Singh, T. Bastow, M. Trigg, *Structural studies of geopolymer by Si and Al MAS-NMR*, Journal of materials science 40 (2005) 3951-3961

[33] P. P. Man, M. J. Peltre, D. Barthomeuf, *Nuclear magnetic resonance study of the dealumination of an amorphous silica-alumina catalyst*, J. CHEM. SOC. FARADAY TRANS., 1990, 86(9), 1599-1602

[34] S. Greiser, G. J. G. Gluth, P. Sturm, and C. Jäger, *29Si27Al, 27Al29Si and 27Al1H double-resonance NMR spectroscopy study of cementitious sodium aluminosilicate gels (geopolymers) and gel-zeolite composites*, RSC Adv., vol. 8, no. 70, pp. 40164–40171, 2018

[35] E. Alvarez-Ayuso, X. Querol, F. Plana, A. Alastuey, N. Moreno, M. Izquierdo, O. Font, T. Moreno, S. Diez, E. Vazquez, M. Barra , *Environmental, physical and structural characterisation of geopolymer matrixes synthesized from coal (co-)combustion fly ashes*, J. Hazard Mater. 154, 175e183

[36] Z. Zhang, H. Wang, J.L. Provis, F. Bullen, A. Reid, Y. Zhu, *Quantitative kinetic and structural analysis of geopolymers. Part 1. the activation of metakaolin with sodium hydroxide*, Thermochim. Acta 539, 23e33

[37] E.N. Kani, A. Allahverdi, J. L. Provis, *Efflorescence control in geopolymer binders based on natural pozzolan*, Cement & Concrete Composites 34 (2012) 25–33

[38] R.R. Lloyd, J. L. Provis, J. S. J. Van Deventer , *Pore solution composition and alkali diffusion in inorganic polymer cement*, Cem Concr Res 2010;40(9):1386–92

[39] H. Szklorzová, V. Bílek, *Influence of alkali ions in the activator on the performance of alkali-activated mortars*, International symposium on non-traditional cement and concrete. Czech Republic: Brno; 2008. p. 777–84.

[40] C. Bobirica˘, J. Shim, J. Pyeon, J. Park, *Influence of waste glass on the microstructure and strength of inorganic polymers*, Ceram. Int. 41 (2015) 13638–13649

[41] S. Ahmed, F. R. Jones, *A review of particulate reinforcement theories for polymer composites*, School of Materials, University of Sheffield, Northumberland Road, Sheffield, UK

[42] R.W. Rice , *Limitations of pore-stress concentrations on the mechanical properties of porous materials*, Journal of Materials Science volume 32, pages4731–4736(1997)

[43] D.D. Ramteke, M. Hujova, D. Galusek, P. Colombo, E. Bernardo, *Extensive reuse of waste glass in geopolymer-like materials*, University of Trencin, FunGlass (Centre for Functional and Surface Functionalized Glass), Slovakia, IIC SAS, Joint Glass centre, Slovakia, University of Padova, Department of Industrial Engineering, Italy

[44] R.A. Fletcher, K.J.D. MacKenziea, C.L. Nicholsona, S. Shimadac, *The composition range of aluminosilicate geopolymers*, Journal of the European Ceramic Society 25 (2005) 1471–1477

[45] P.S. Singh, M. Trigg, I. Burgar, T. Bastow, *Geopolymer formation processes at room temperature studied by ^{29}Si and ^{27}Al MAS-NMR*,Materials Science and Engineering A 396 (2005) 392–402

[46] S. Luhar, T.W. Cheng, D. Nicolaides, I. Luhar, D. Panias, K. Sakkas, *Valorisation of glass waste for development of Geopolymer composites*

– *Mechanical properties and rheological characteristics: A review*, Construction and Building Materials 220 (2019) 547–564

[47] A. Palomo, P. Krivenkob, I. Garcia-Lodeiroa, E. Kavalerovab, O. Maltsevaa, A. Fernández-Jiménezа *A review on alkaline activation: new analytical perspectives*, Materiales de Construcción, ISSN-L: 0465-2746

[48] D.R.M. Brew, K.J.D. MacKenzie, *Geopolymer synthesis using silica fume and sodium aluminate*, J Mater Sci (2007) 42:3990–3993

[49] S. Greiser, P. Sturmb, G.J.G. Gluthb, M. Hungerc, C. Jägera, *Differentiation of the solid-state NMR signals of gel, zeolite phases and water species in geopolymer-zeolite composites*, Ceramics International 43 (2017) 2202–2208

[50] H. Xu, J.S.J. Van Deventer, *The geopolymerisation of alumino-silicate minerals*, Int. J. Miner. Process. 59 (2000) 247–266

[51] H. Xu, J.S.J. Van Deventer, *Microstructural characterisation of geopolymers synthesised from kaolinite/stilbite mixtures using XRD, MAS-NMR, SEM/EDX, TEM/EDX, and HREM*, Cement and Concrete Research 32 (2002) 1705–1716

[52] B.S. Lartiges, J.Y. Bottero, L.S. Derrendinger, B. Humbert, P. Tekely, H. Suty, *Flocculation of Colloidal Silica with Hydrolyzed Aluminum: An ^{27}Al Solid State NMR Investigation*, Langmuir 1997, 13, 147-152